PERFORMANCE EVALUATION OF ROOF-MOUNTED PHOTOVOLTAIC MODULES IN SELECTED RURAL SECONDARY SCHOOLS IN NORTHERN AND EASTERN UGANDA

BY

BETTY AUMA

18/U/GMSP/19491/PD

A DISSERTATION SUBMITTED TO THE DIRECTORATE OF RESEARCH AND GRADUATE TRAINING IN PARTIAL FULFILMENT OF THE REQUIREMENTS FOR THE AWARD OF THE DEGREE OF MASTER OF SCIENCE IN PHYSICS OF

KYAMBOGO UNIVERSITY

OCTOBER, 2025

DECLARATION

I, **Betty Auma** do declare that this study was carried out by me and its findings have never been submitted to any other university or academic institution for the purpose of an academic award.

Date: ……..

Signature: ……..

APPROVAL

This is to certify that this study by **Betty Auma** entitled **'Performance evaluation of roof-mounted photovoltaic modules in selected rural secondary schools in Northern and Eastern Uganda'** was carried out under our close supervision and is hereby approved for submission to the Directorate of Research and Graduate Training and the Senate of Kyambogo University.

Supervisors

1. Dr. Okullo Michael

Signature: …….. **Date:** ……..

2. Dr. Oyirwoth Patrick Abedigamba

Signature: ……... **Date:** …….

DEDICATION

I dedicate this dissertation to my father, Mzee Deus Celestino Lem and my lovely mother, Beatrice Dues Celestino Lem.

ACKNOWLEDGEMENT

I wish to express my heartfelt gratitude to my principal supervisor, Dr Michael Okullo, for his initiative on photovoltaics in the department and his indispensable guidance right from the beginning of the study to the end.

I am also greatly indebted to Dr Oyirwoth Patrick Abedigamba, my second supervisor, for his valuable advice and the deliberations we always had in the processes of performing experiments and writing the report.

Contributions made by my classmates, especially Mr Seba from Tanzania, cannot be forgotten. Thanks a lot for taking me through the analysis of the results.

I am very happy to express my appreciation to all members of the Department of Physics of Kyambogo University for their hospitality and moral support rendered to me.

In a special way, I recognize the input from my betrothed, Mr Ekwang Denis and our lovely children (Daniella, Jessica, Emmanuella, and Isaac). Your courage and patience during times when I was concentrating on this work greatly contributed to the success and ultimate completion of the work.

All friends who, in one way or another, rendered to me technical advice accompanied with words of consolation. Thank you.

TABLE OF CONTENTS

LIST OF FIGURES

LIST OF TABLES

LIST OF ABBREVIATIONS AND ACRONYMS

CAA	Communications and Accessories
ERT	Energy for Rural Transformation
EVA	Ethylene Vinyl Acetate
FF	Fill Factor
FTV	Forward Tunneling Voltage
HS	High School
ICT	Information Communication Technology
IEC	International Electrotechnical Commission
LID	Light-Induced Degradation
MAAF	Ministry of Agriculture, Animal Industry and Fisheries
MEMD	Ministry of Energy and Mineral Development
MMP	Maximum Power Point
MoES	Ministry of Education and Sports
MoFPED	Ministry of Finance, Planning and Economic Develo`pment
MOH	Ministry of Health
MoLG	Ministry of Local Government
MOWE	Ministry of Water and Environment
OPC	Operating Conditions
PID	Potential-Induced Degradation

PV	Photovoltaic
STC	Standard Testing Condition

ABSTRACT

This study focused on the performance of roof-mounted photovoltaic modules in selected rural secondary schools in Northern and Eastern Uganda. The Ministry of Education and Sports installed these modules under the Energy for Rural Electrification Project II to address the electrical power problem in rural secondary schools. The study was carried out using three objectives, namely, to perform visual inspection using the International Electrotechnical Commission (IEC) guidelines, to determine the module maximum power using the I-V characterization technique and to determine the conversion efficiencies of the modules. The modules studied are installed at Orungo SS, Katine SS, Akii Bua Comprehensive SS and Adwari SS. In the visual inspection done, most of the modules had green leakage, water ingress, discolouration, cracks, snail trails, scratches, black spots, dust, debris, bird droppings, burnt spots on diodes, rust, broken sealant, and broken cell interconnects. Experimental data were collected using the FTV200 I-V tracer. Findings revealed that the maximum power output of the PV modules was higher after washing the modules. The modules at Orungo High School produced the highest power (62 W), while the modules at Akii Bua Comprehensive School produced the lowest (34.5 W). The drop in module efficiencies as compared to the manufacturer's efficiency, with degradation taken into account, was found to be highest for the modules at Akii Bua Comprehensive School (11.3%) and lowest for the modules at Orungo High School (5.5%). Despite taking degradation into account, all the modules were found to have a significant drop in their power output as well as efficiencies.

CHAPTER ONE: INTRODUCTION

1.0 Background to the Study

Generation of electric power from photovoltaic (PV) modules in Uganda is currently becoming increasingly attractive as hydroelectric power continues to be costly and limited in supply. Most rural secondary schools have computer laboratories established, and these laboratories are equipped with solar modules to provide power to run the computers. Photovoltaic modules perform optimally and live longer if the cells in a module or modules in a string are free from current mismatch, soiling, shading, bird droppings, cracks, scratches and snail trails. Renewable energy resources, such as solar energy, contribute to 8% of the total energy consumed in Uganda [1]. This contribution is on the rise with the current government energy policy, favouring renewable energy use [2].

In 2013, the government of Uganda implemented a project, Energy for Rural Transformation phase II (ERT II), as a follow-up of ERT I. The project had three components: Rural Energy structure, Information Communication Technology, Energy Development, cross-sectoral links, and impact monitoring. Funds for these implementations were channelled to the accounts of seven implementing ministries: Ministry of Energy and Mineral Development (MEMD), Ministry of Health (MOH), Ministry of Water and Environment (MOWE), Ministry of Agriculture, Animal Industry and Fisheries (MAAF), Ministry of Education and Sports (MoES), Ministry of Finance, Planning and Economic Development (MOFPED) and Ministry of Local Government (MOLG) [3]. The Ministry of Education benefited from this project and installed photovoltaic modules in about 560 rural secondary schools in more than 40 districts across the country. This project was initiated in support of the introduction of Information and Communication Technology (ICT) in the Education system of Uganda [4]. ICT was integrated into the Education system of Uganda to improve the engagement and innovativeness of learners by the use of computers and the internet, with good knowledge retention. Roof-mounted PV modules, which convert solar energy into electricity, were installed in rural secondary schools across the country to generate electrical power for running these computers.

The rooftops of buildings are the common mounting places for Photovoltaic modules as they appear to present a better module exposure to solar radiation, and provide safety and security of

the modules. However, since the modules are high up, little attention is usually paid to them in terms of maintenance, hence making the modules susceptible to current mismatch [5].

Photovoltaic modules may have identical electrical properties at the time of manufacture; however, during transportation or field exposure, the modules may experience mechanical loads like transport vibrations, installation loads and loads resulting from wind, hailstorms and heavy rainfall, which may cause visible defects on the module glass and frame. Due to the fragile nature of crystalline silicon PV cells, the modules need to be handled with great care, especially during transportation and installation, as they are susceptible to developing cracks.

Additionally, weather conditions are always randomly changing, causing variations in the module ability to charge storage batteries. This assumption may be wrongly attributed to the changing weather conditions, yet the problem may originate from the modules. When PV modules do not perform as expected, the ICT curriculum may not be well implemented and integrating methodologies that use computer-like projecting work on the screen will be rendered non-functional; hence, teaching and learning requiring the use of ICT integrations will be halted. Performance evaluation of roof-mounted PV modules installed by the MoES with the objective of improving ICT integration in the education system in Uganda is therefore essential to assess the functionality of the modules in terms of the module's efficiency, so that remedial measures could be put in place if required.

1.1. Statement of the Problem

Information and Communication Technology (ICT) play a critical role in enhancing teaching and learning in Uganda's education system today. However, when ICT was first introduced in secondary schools in 2013, the lack of reliable electrical power to operate the necessary equipment was identified as a major constraint [4]. To address this challenge, the Ministry of Education and Sports (MoES), with financial support from the Government of Uganda under the Energy for Rural Transformation Phase II (ERT II) project, installed photovoltaic (PV) modules in selected secondary schools across the country.

Despite this intervention, a report by the Auditor General of 2014 in a survey of ERT installations revealed performance challenges in several beneficiary schools, including Katine SS, Akii Bua Comprehensive SS, Orungo High School and Adwari SS. These schools reported immediate lamp

failures, which significantly reduced daily lighting hours due to ageing batteries or design limitations, and declining PV output over time caused by factors such as module soiling, thermal stress, and encapsulant degradation.

Given these issues, there was a critical need to evaluate the performance of the roof-mounted PV modules in these schools. Therefore, this study sought to provide valuable feedback to the MoES and other stakeholders, thereby informing future strategies for sustainable ICT integration and energy provision in Uganda's education sector.

1.2. General Objective

The general objective of the study was to evaluate the performance of roof-mounted photovoltaic modules in selected rural Secondary schools in Northern and Eastern Uganda.

1.3. Specific Objectives of the Study

i. To perform visual inspection using the International Electrotechnical Commission (IEC) PV visual inspection guidelines.

ii. To determine the module maximum power using the Current–Voltage characterization technique.

iii. To determine the conversion efficiencies of the modules

1.4. Scope of the Study

This study was carried out on polycrystalline silicon roof-mounted PV modules connected to the computer Laboratories installed in rural secondary schools in Eastern and Northern Uganda. Schools with similar modules and power ratings were randomly selected. The PV modules manufactured by CAA Communications and Accessories AG, model SL110CE-18P, of power rating 110 W each, were assessed. The study was carried out on two (2) modules connected in parallel, each in a string installed at Akii Bua Comprehensive Secondary School and Adwari Secondary School, Northern Uganda, Katine Secondary School and Orungo High School, Eastern Uganda. Visual inspection was done on the modules using the IEC guidelines. The FTV200 I-V tracer was used to measure the different electrical parameters: short circuit current, open circuit voltage, maximum power and efficiency of the modules before and after washing the modules with

a sponge and clean water.

1.5. Significance of the Study

This study provides critical feedback to the MoES so that informed decision-making, resource allocation and strategic planning can be made. The feedback loop helps the MoES to continuously improve and expand its renewable energy initiatives, ultimately contributing to better educational environments and sustainable development goals.

This study sets a foundation for further research. It offers valuable data for systems designers and researchers interested in the performance of PV modules in Uganda. The information can be used to improve future designs and implementations, contributing to the overall advancement of solar technology in the region.

The study would also help the government of Uganda to achieve NDP 3 project development goal no.9, set to increase access to stable, reliable and affordable energy. UN Sustainable Development Goal No. 7: ensuring access to affordable, reliable and modern energy for all.

With the gaps in this study properly addressed, the generation of electricity using PV modules can be a good option for schools, as it helps to reduce the utility cost.

CHAPTER TWO: LITERATURE REVIEW

2.0 Introduction

Review of related studies on PV module structure, visual inspection, PV modules parameters, solar irradiance effect, thermal effects, PV modules degradation, PV modules current-voltage characteristics and identification of faults and failures in the PV modules were handled.

2.1 The PV Module Structure

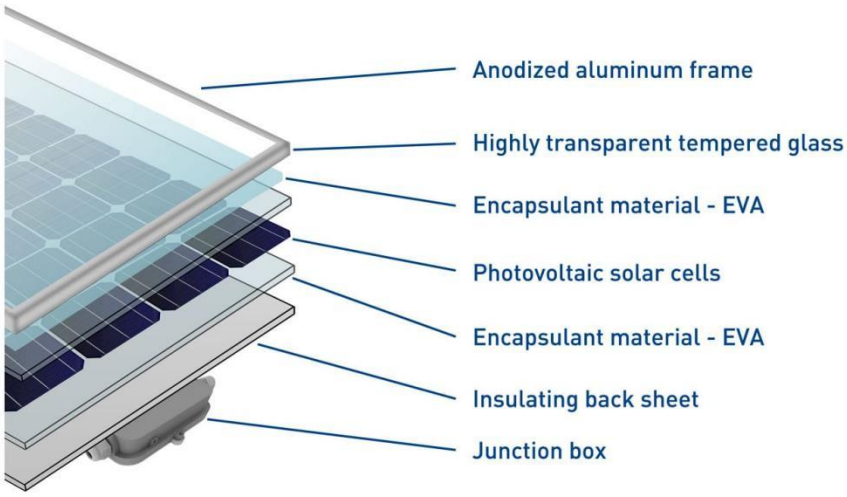

Figure 2.1: The structure of a PV module by Pathy et al [6].

A Photovoltaic (PV) module, also called a solar module, is a collection of photovoltaic cells that convert sunlight into electrical energy. PV modules typically consist of Photovoltaic (PV) cells, which are the core components of the module, responsible for converting sunlight into electricity Figure 2.1 [7]. PV cells are made from semiconducting materials like silicon [8] and are arranged in a grid-like pattern on the surface of the module. It also consists of a glass or tempered glass cover, which is the top layer of the module to protect the PV cells from environmental factors like weather, debris, and UV radiation [8].

PV modules are built with a back sheet, which is a thin, flexible plastic sheet made of Tedlar, a

type of polyvinyl fluoride (PVF), which provides additional protection and prevents moisture and air from entering the module [9]. It is made up of encapsulant, a transparent plastic or resin material that seals the gap between the PV cells and the Tedlar back sheet [10], ensuring that moisture and air do not enter the module, with a frame which provides structural support to the module and helps to secure it to the mounting system [11]. The frame is typically made of aluminium or anodized aluminium to provide a corrosion-resistant and lightweight structure. At the same time, the whole pattern on the back of the module allows for easy installation and wiring [11]. PV modules also have wiring, which connects the individual PV cells within the module to each other and to the junction box [12].

2.2 PV Module Performance Parameters

In the context of photovoltaic (PV) modules, performance parameters refer to various metrics that measure the efficiency and effectiveness of a PV Module [13]. These parameters are used to evaluate performances and to identify areas for improvement [14]. Among the module performance parameters are short circuit current, open circuit voltage, Maximum Power output (Pmax), Efficiency (η), solar irradiance and temperature [15]. These performance parameters are important for evaluating the performance of individual modules, strings, and for optimizing their operation and maintenance over time, as expounded on in the following sections.

2.2.1 Short Circuit Current (I_{SC})

When the voltage across the circuit is equal to zero, the short circuit current, I_{SC} is obtained on condition that the solar cell is short-circuited**.** Therefore, when we set V = 0, then

$$I = I_{SC} \tag{2.1}$$

The short circuit-current from a solar module depends linearly on light intensity. However, this effect does not provide an increase in efficiency because the incident power also increases linearly with concentration [16]. For an ideal module, the maximum current, I_{max} value gives the total current produced at the beginning of a forward bias sweep in the solar cell by photo excitation. Ideally,

$$I_{SC} = I_{\max} = I_L \tag{2.2}$$

2.2.2 Open Circuit Voltage V*oc*

The maximum voltage available from a solar cell is the open circuit voltage, which occurs at zero current. The expression for V_{oc} is given by equation (2.3) [17], which reflects how the saturation current I_0 dependence on the V_{OC} of the solar cell and the light generated current I_L. Since the light generated current has a small variation, the major parameter that affects the open circuit voltage is the saturation current, which depends largely on recombination in the solar cell. V_{OC} is therefore a measure of recombination in the solar module [18].

$$V_{oc} = \frac{nkT}{q} \ln\left(\frac{I_L}{I_0} + 1\right) \tag{2.3}$$

Where, Voc is the open-circuit voltage

n is the ideality *factor*

k is the Boltzmann constant

T is absolute temperature

q is the elementary chargeI_L

I_L *is* photogenerated current (or light-generated current)

I_0 *is* the reverse saturation current (dark saturation current)

2.2.3 Maximum Power (P_{max})

On the I-V curve shown in Figure 2.1, the product defined as $P = VI$ gives the rate of work done delivered by the solar cell at a particular coordinate [19]. At another point, there is a maximum value for this product. This value is the maximum power delivered by the solar module. The value of voltage that gives this value is the voltage at maximum power, V_{mp}, while the amount of current that gives maximum power is the current at maximum power, I_{mp}. Following Lorenzo [18], maximum power is given by Equation (2.4).

$$P_{max} = Imp \times Vmp \tag{2.4}$$

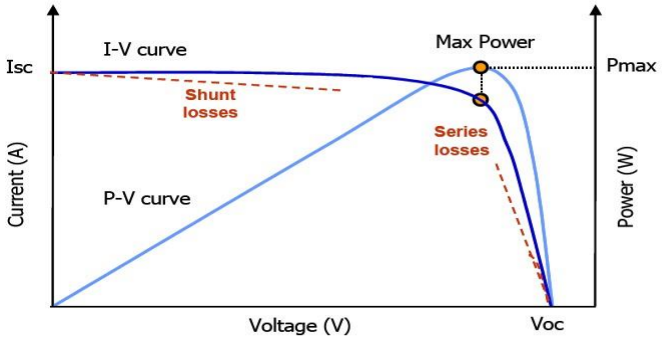

Figure 2.2: Sketch graph of current-voltage characteristics of a solar module.

It is important to determine I_{mp} and V_{mp}. These would be read and noted directly from the current and voltage axes (Figure 2.2) and used in the calculation of maximum power of the module as in Equation (2.4).

2.2.4 Efficiency (η)

The maximum power generated by the solar irradiance that is reaching the PV module defines the Efficiency of the system [20]. Thus, if G is the irradiance, A, the area of the PV module, then efficiency (η) is given by:

$$\eta = \frac{P_{\max}}{G \times A} \text{ x } 100\% \tag{2.5}$$

The operating temperature and solar energy received determine the efficiency of a photovoltaic system [21]. For polycrystalline silicon PV, efficiency of over 17 % has been reported [22]. However, energy conversion efficiencies of around 40 % have been recently achieved in laboratories using I-V semiconductor compounds as PV material. Currently, the photovoltaic efficiency of silicon crystalline solar modules is up to 22 % [23]. Dust accumulation on PV modules significantly affects their performance [24].

2.2.5 Shunt and Series Resistance in PV Modules

Owing to resistances referred to as series and shunt resistance, PV modules suffer significant power losses [25]. Shunt resistance is any parallel high-conductivity paths across the solar cell p-n junction [26]. Shunt resistance arises mainly from leakage losses across the p-n junction. These losses are enhanced by the presence of defects and impurities around the edge of the cell, which provide alternative paths [27]. The alternative paths divert currents away from the intended load. The detrimental effects of shunt resistance on the module performance have been reported by the low intensity [28]. A model for shunt resistance (R_{sh}) and series resistance (R_S) are shown in Figure 2.2.

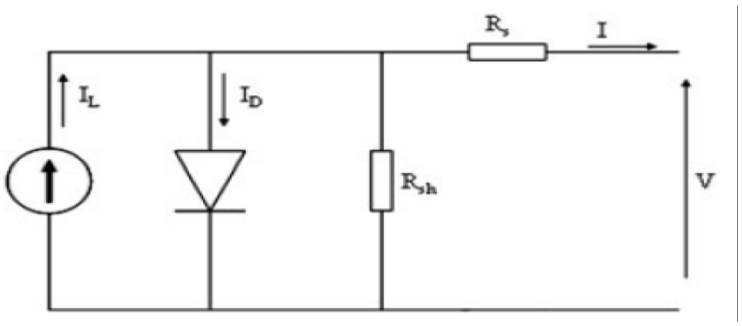

Figure 2.3: Series and shunt resistance [28].

Figure 2.3 below shows the effects of R_{sh} on the I-V characteristic of a PV module as investigated by Macabee and Van Dyk [25] [28].

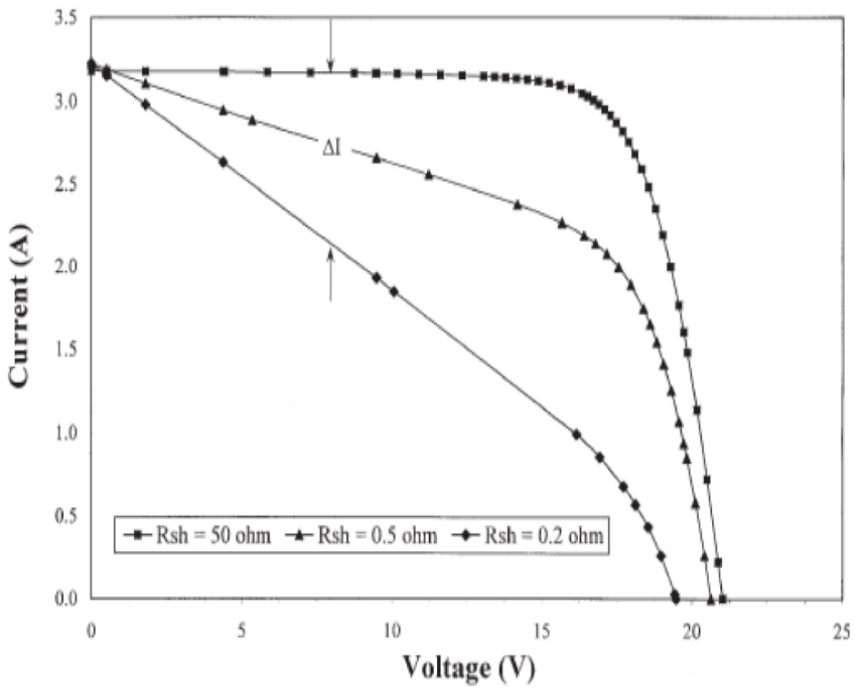

Figure 2.4: Effects of variations of shunt resistance on performance parameters [28].

A small shunt resistance significantly reduces V_{OC} and the Fill Factor (FF) of the module. At I_{sc} the effect of low R_{sh} is minimal because current flows mainly through the external circuit. For a module to operate more efficiently, R_{sh} must be infinite so that currents are not led away from the intended load [29].

On the other hand, series resistance is usually ascribed to the bulk resistance of the semiconductor material of the module, the bulk resistance of metallic interconnections, and the contact resistance between the semiconductor and the metallic contacts [30]. These elements derive their resistivity from the manufacturing technology [31]. The effects of R_S on the simulated I-V characteristic of a PV module discussed by [32] are shown in Figure 2.4 for a 36-series-connected solar cell module.

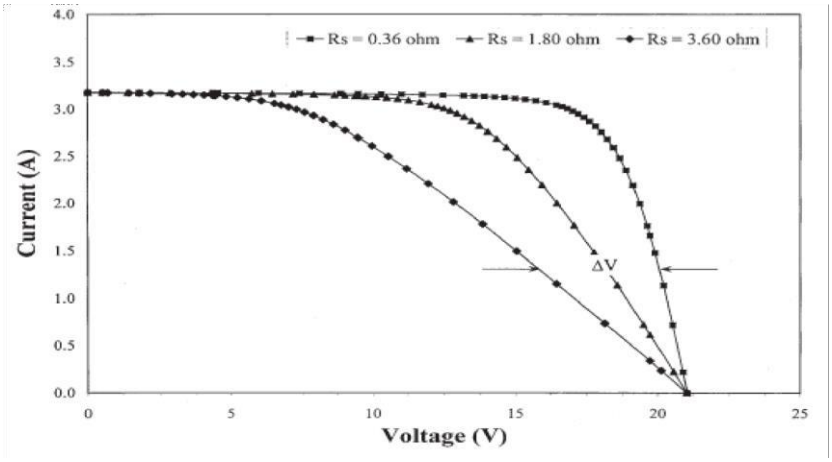

Figure 2.5: Effects of variations of series resistance on performance parameters [28].

From Figure 2.5, a large series resistance severely decreases the Fill factor without affecting the open circuit voltage of the module. The value of V in the I-V characteristic is equal to the current at that point, multiplied by the series resistance [32]. The increase in series resistance reduces the voltage output and fill factor of the module, thereby affecting its performance quality. [28]. I_{sc} starts to decrease for higher values of Rs [33].

2.2.6 Fill Factor (FF)

The open circuit voltage V_{oc} and short circuit current I_{sc} are the maximum voltage and current, respectively, that may be drawn from a solar cell. Unfortunately, such an operating point in a solar cell is not attainable. At each of these coordinates, the power from the solar cell is zero. The fill factor (FF) together with V_{oc} and I_{sc} presents a realistic definition of maximum power from a solar cell. Precisely, FF is defined as the ratio of the maximum power from a solar cell to the product of V_{oc} and I_{sc}. [34]

$$FF = \frac{P_{max}}{I_{sc} \times V_{oc}} \tag{2.6}$$

Graphically, FF is the area of the largest possible rectangle within the I-V curve divided by the product Isc × Voc, depicted in Figure 2.6.

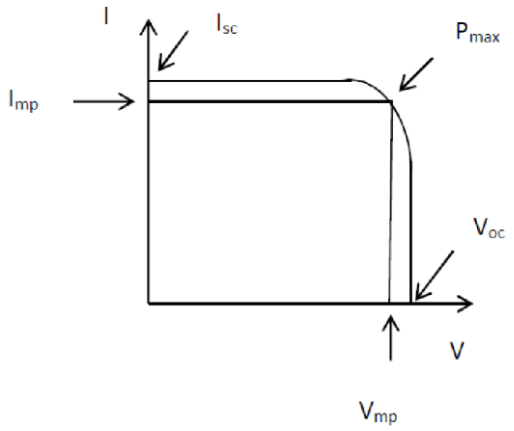

Figure 2.6: I-V characteristics of a solar cell showing fill factor [35].

Shockley et al [36] have derived FF as an implicit function of open circuit voltage

$$FF = \frac{v_m^2}{(1 + v_m - \exp(-v_m))(v_m + \ln(1 + v_m))} \tag{2.7}$$

where, $V_{oc} = v_m + In\ (1 + v_m)$

v_m: is a variable, like velocity, or normalized speed, it's raised to powers, used in exponential and logarithmic functions, and it's positive or negative.

exp $(-v_m)$: This is the exponential decay term. As v_m increases, this term decreases rapidly.

ln $1 + v_m$: Natural logarithm of $1+v_m$ grows slowly with increasing v_m, and ensures the argument of the log is always positive.

The normalized open circuit voltage v_{oc} is defined as,

$$v_{oc} = V_{oc}\frac{q}{KT}, \tag{2.8}$$

Then, an empirical relation for FF involving open circuit voltage is given by

$$FF_o = \frac{v_{oc} - \ln(v_{oc} + 0.72)}{v_{oc} + 1} \tag{2.9}$$

where FF_0 is the Fill factor at zero series resistance r_s, defined as $r_s = \frac{R_s}{R_{CH}}$. The quantity

$R_{CH} = \frac{V_{oc}}{I_{sc}}$ is called the characteristic resistance [37].

The loss in Fill factor due to series resistance is given by:

$$FF = FF_0 (1 - r_s) \tag{2.10}$$

Equations (2.8), (2.9) and (2.10) were found to be valid for $v_{oc} > 10$ and $r_s < 0.4$ [37] .

Shunt resistance effects on fill factor were estimated as;

$$FF = FF_0 \left[1 - \frac{(v_{oc} + 0.7)\, FF_o\, (1 - r_s)}{v_{oc} \times r_{sh}}\right] \tag{2.11}$$

where the normalized shunt resistance is defined as $r_{sh} = \frac{R_{sh}}{R_{CH}}$. Equation 2.13 is valid for $v_{oc} > 10$ and $r_{sh} < 2.5$. The effect of combined series and shunt resistance is obtained by replacing FF_o of Equation (2.11) by FF of Equation (2.10), so that we have;

$$FF = FF_o\, (1 - r_s) \left[1 - \frac{(v_{oc} + 0.7)}{v_{oc}} \frac{FF_o\, (1 - r_s)}{r_{sh}}\right] \tag{2.12}$$

In general, the value of FF in Equation (2.12) varies between 0.5 and 0.82, largely depending on the solar module material and technology used [38]. The FF value close to 1 is known to indicate high quality of the solar module[[39]. The Series resistance represents the internal resistance within the PV module. It arises from the conductive paths within the semiconductor material, metal contacts, and interconnections. It decreases the fill factor (FF) and efficiency of the solar module, reduces the maximum power output, and shifts the current-voltage (IV) curve downward, affecting the Shunt resistance, which represents the resistance parallel to the PV cell. It is associated with leakage paths or defects that affect the performance of the modules. Series resistance has a greater effect on performance at high light intensity.

2.3 Solar Irradiance Effects

It is asserted by Makrides G [39] that the most important environmental factor that determines the functionality of PV modules is the amount of irradiance. The operating voltage and current of a PV device depend logarithmically and linearly, respectively, on irradiance. Different scholars observe that, when irradiance is low, the efficiency and performance of the PV modules, which

are dependent on the technology of each PV system, decrease. The solar irradiance effect was studied using an outdoor evaluation technique. Values of temperature at Standard Test Condition (STC) were calculated at a gain cell using the manufacturer's temperature coefficients. I-V curves were obtained and used to determine the efficiency of the modules. The efficiency of the modules obtained from the I-V curves at each value of irradiance level was evaluated and compared [40].

2.4 Thermal Effects

It has been noted that PV modules that are installed in warm climates have module temperatures above 25 ℃ [41], and this results in a reduction in the efficiency of the PV system. Temperature coefficients measured by manufacturers using indoor laboratory techniques are the only parameters which describe the electrical characteristics of a PV module with the operating temperature [42]. At controlled STC irradiance, the I-V curves of the device are obtained. The differences in either the voltage, current or power of the module are dependent on temperature [43]. PV modules operate under varying conditions, including temperature and irradiance. As temperature increases, the efficiency of PV modules tends to decrease due to increased losses (like increased Rs) and reduced open-circuit voltage. Irradiance affects the overall power output of PV modules. Higher irradiance leads to higher power generation.

2.5 PV Degradation

Photovoltaic modules at the time of installation perform optimally, but due to changes in the climate and other factors, their performance gradually deteriorates throughout the years [19]. The degradation of the modules results from the ageing of the material, which leads to performance loss, loss due to corrosion of the contacts, which results from water vapour ingress, failure mechanisms of the cell, weakening of the materials used for packaging, breakage of interconnects, cell cracking, manufacturing defects, bypass diode and encapsulant failures, and then delamination [44]. Despite being considered reliable devices, PV modules can experience failures and extreme degradations. Degradation mechanisms include: Light-induced degradation (LID), which is a reversible effect observed in certain types of solar cells, where initial exposure to light reduces efficiency. Potential-induced degradation (PID), a Voltage stress that can lead to performance degradation [45]. Mechanical stress: Thermal cycling, wind, and other environmental factors can cause microcracks or delamination. Exposure to moisture and harsh environments can lead to

corrosion of cell components. Non-uniform illumination can cause localized heating and damage called a hot spot [46]. Understanding these failure modes helps improve module design and reliability.

2.6 PV Module Faults and Failures

Photovoltaic (PV) modules are often not free from defects and therefore require regular monitoring to ensure optimal performance. Crystalline silicon PV modules typically exhibit a power degradation rate of approximately 0.8% per year [17]. Faults in PV modules can be broadly categorized into early failures, intrinsic or random failures, and deterioration over time. Early failures usually occur during the initial stages of installation and operation, whereas intrinsic failures and deterioration develop as the modules are exposed to real-world environmental conditions.

One common factor affecting PV performance is the accumulation of particles on the module surface. These deposits interfere with illumination by attenuating and scattering incoming light, significantly reducing the module's efficiency [47]. The extent of this interference depends on the particles' composition, density, and size [48]. Such contamination accelerates degradation and ultimately shortens the module's service life.

Several components of PV modules are particularly prone to failure. These include the junction box, glass cover, cell interconnections, and instances of delamination [44]. The durability of junction boxes and glass frames remains a significant concern [49]. Inadequate design of junction boxes can allow moisture ingress, leading to corrosion of interconnects and failures in wiring or soldering issues that often result in internal arcing.

Studies indicate that approximately 2% of PV modules fail to meet manufacturer warranty standards after some time in the field. These failures can be attributed to a combination of factors, including manufacturing defects (e.g., faulty interconnections), poor transportation and handling, incorrect installation, and adverse environmental conditions, all considered major causes of extrinsic failure [12]. Over time, such defects can cause overheating, which in turn leads to cracks and hotspots, further diminishing performance and raising electrical safety concerns [49]. Additionally, there are other less common defects that are difficult to categorize, making diagnosis and classification more challenging.

Transportation-related issues, such as shocks and vibrations, can result in glass breakage and lamination damage [50]. However, many of these failures are not visually apparent and cannot be easily detected through standard power output measurements. To identify such hidden defects, I-V (current-voltage) characterization techniques using plotted curves are often employed [51].

2.7 PV Modules Current – Voltage Characteristics

The current-voltage (I-V) characteristic of a photovoltaic (PV) module describes the relationship between the current output and its voltage output under various conditions [52]. The open-circuit voltage, V_{OC} is the maximum voltage that can be measured across the PV module when it is not connected to any load or circuit [53]. V_{OC} is typically measured at a temperature of 25 °C (77 °F) and a solar irradiance of 1,000 W/m² [53]. At the same time, the short-circuit current I_{SC} is the maximum current that can be drawn from the PV module when it is short-circuited, meaning there is zero resistance between the positive and negative terminals. I_{SC} is also measured at a temperature of 25 °C (77°F) and a solar irradiance of 1,000 W/m² [54].

The I-V curve typically has three regions; one of which is the knee region where the current increases rapidly as the voltage decreases, indicating that the module is operating in a high-efficiency region [55], saturation region where, the current approaches its maximum value I_{SC} as the voltage approaches zero, indicating that the module is operating at maximum power point [56] and the reverse bias region where the current decreases rapidly as the voltage increases, indicating that the module is operating in a low-efficiency region [56].

On the I-V curve, the Maximum Power Point (MPP) is a point where the power output of the PV module is maximum[57]. Fill factor (FF), on the other hand, measures how well the PV module approaches its maximum power point under standard test conditions [58]. At the same time, open-circuit voltage drop shows the difference between V_{OC} and V_{mpp}, which represents the voltage drop across internal resistance [53]. However, current–voltage (I-V) characteristics in PV modules may be determined by temperature, irradiance, shading, cell quality and technology, taking, for instance, increasing temperature in PV modules reduces V_{OC} and increases I_{SC}, increasing irradiance increases V_{OC} and I_{SC}, shading reduces V_{OC} and $I_{SC,}$ while different cell technologies and qualities can affect I-V characterization [53].

The current-voltage characteristics of the PV modules are simply the I-V curve of a p-n junction

(solar in darkness) superposed [59]. Even in the dark, a small electric current is generated in a solar cell, that is, when no photons are directed onto the device. The cell would be acting like a simple diode, with the I-V curve described by Equation (2.13) [60].

$$I_D = I_0 \left(\exp\left(\frac{qV}{nkT} \right) - 1 \right) \tag{2.13}$$

where I_0 is the reverse saturation current, k is the Boltzmann constant, the junction temperature is T, and n is the ideality factor, which depends on the type of semiconductor used, and usually takes on a value of 1 or 2. When light strikes the module, there is an increase in power generated [61], and the I-V curve shifts away from the origin at the same time. The greater the light intensity, the greater the shift away from the origin. This can be attributed to the random generation of electrons and holes within the depletion region of the device, which are immediately swept away by the built-in electric field. A photon-generated current I_L results in opposition to the dark current I_D, Figure 2.7.

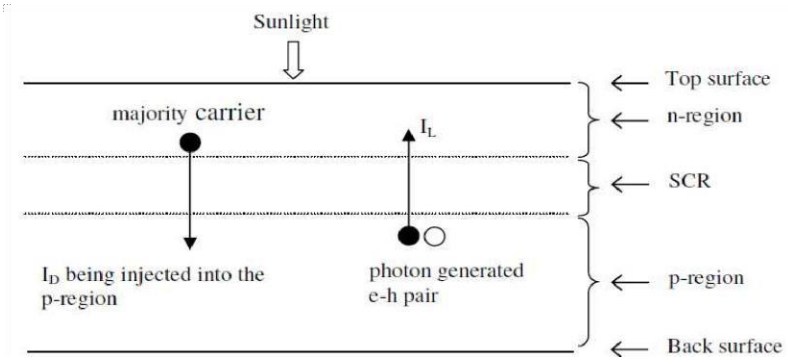

Figure 2.7: Current production in a solar module [62].

The open circle represents holes, and the shaded circles represent electrons. At this state, the I-V characteristics are governed by the modified diode Equation (2.14) [36].

$$I = I_0 \left[\exp\left(\frac{qV}{nKT} \right) - 1 \right] - I_L \tag{2.14}$$

According to Sze [63], the current source parallel to the diode is the constant equivalent circuit as

shown in Figure 2.8. I is the photogenerated current and I_D, the dark current of the solar cell.

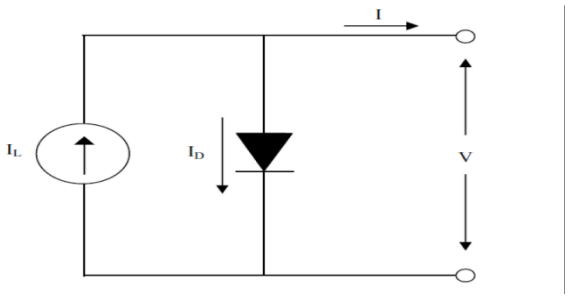

Figure 2.8: Single diode equivalent circuit of an ideal solar cell [64].

However, the double-exponential model better describes the current-voltage characteristics of the PV modules [33].

$$I = I_{ph} - \left[I_{01} \left(\exp\left(\frac{qV_j}{n_1 kT} \right) - 1 + I_{02} \left(\exp\left(\frac{qV_j}{n_2 kT} \right) - 1 \right) \right) \right] - \frac{V_j}{R_{sh}} \tag{2.15}$$

where I_{01} and n_1 are the pre-exponential constants and ideality factor resulting from the recombination in quasi-neutral (or bulk) regions respectively, I_{02}, n_2 result from the rearrangement in the space charge (or the depletion) region of the cell, I_{ph} is the photo generated current, I_0 the reverse saturation current, V_j the voltage developed or dropped across the junction, n is the ideality factor, k is the Boltzmann constant, T the temperature of the cell and V_f is the terminal voltage, series and shunt resistance are R_s and R_{sh}, respectively.

CHAPTER THREE: RESEARCH METHODOLOGY

3.0 Introduction

This chapter explains the research design, visual inspection procedure, determination of the module maximum power output, efficiency and comparison of the experimentally measured module efficiency with the manufacturer's module efficiency, giving the effect of the different parameters on the efficiency of the modules. Data were collected from PV Modules installed in selected rural secondary schools in Northern and Eastern Uganda.

3.1 Research Design

This study involved an experimental method of data collection and quantitative statistical analysis of data obtained using the FTV200 I-V tracer on two polycrystalline photovoltaic modules in a string, Figure 3.1, each of 110 W. The two modules are in parallel in each string installed in a school, which were labelled A and B before washing and A_w and B_w after washing. Each string was labelled AB before washing and AB_w after washing. These modules were installed in 2013, eleven years old by 2024 [11].

Figure 3.1: General arrangements of modules in a string.

The manufacturer's performance parameters are presented in Table 3.1.

Table 3. 1: A summary of manufacturer's module performance parameters.

Parameters	Specification	Units
Open circuit voltage	21.77	V
Short circuit current	6.52	A
Current at maximum power	6.09	A
Voltage at maximum power	18.05	V
Maximum power	110	W

3.1. Visual Inspection Procedure

Visual inspection was done on each polycrystalline PV module in a string installed on top of the roof in each of the selected secondary schools in line with the International Electrotechnical Commission (IEC) guidelines. The International Electrotechnical Commission (IEC) develops and publishes IEC standards, which are based on a global consensus [65]. These standards cover various aspects related to electrical and electronic products, including electrical safety, labelling, performance, and test methods [66]. It provides instructions, guidelines, rules, or definitions that are used to design, manufacture, install, test, certify, maintain, and repair electrical and electronic devices and systems [67]. This guide was used to inspect PV modules at Orungo High School, Adwari SS, Akii Bua Comprehensive SS and Katine Secondary Schools.

3.3 Determination of the Module Maximum Power using the Current-Voltage Characterization Technique

3.3.1 Measurement of Short Circuit Current and Open Circuit Voltage

FTV200 I-V Tracer in Figure 3.2 and schematic diagram Figure 3.3 were used in the measurement of short circuit current and open circuit voltage.

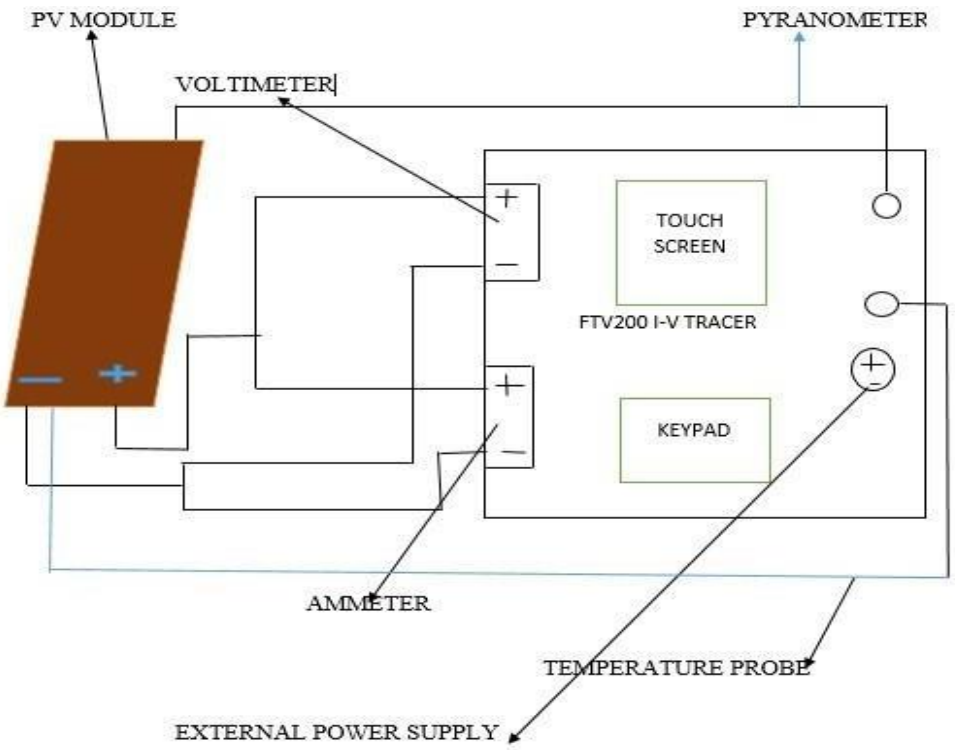

Figure 3:2: Schematic diagram for the experimental set-up.

Figure 3.3: I-V Tracer connected to the modules at Orungo High School.

The pyranometer connected to the I-V Tracer was used to measure solar irradiance, and the thermocouple connected and placed at the back of the module, as shown in Figure 3.3, to measure

the module temperature during the experiment. Solar radiation was measured simultaneously with the I-V characteristics of the PV module, already inclined to ensure maximum exposure to the solar radiation.

The modules were connected in parallel to obtain the maximum yield of current according to the number of modules in a string. Using the I-V tracer, the respective parameters of the modules and strings were measured, recorded and used to extract the I-V curves.

Measurements were done for individual modules and strings before and after cleaning the modules. The modules were washed with clean water using a sponge to remove dust and debris accumulated on the modules, which might reduce the insolation absorbed by the solar cell [67]. Values of open-circuit voltage (Voc) and short-circuit current (I_{sc}) were extracted from the I-V curve and data processed using the FTV200 I-V tracer software and data analysed using Excel and Origin 6.0.

3.3.2 Normalization of Voc and Isc Obtained

The values of open circuit voltage obtained were normalized since it is dependent on measured Temperature, T_m and measured Solar irradiance, G_m [68]. Normalization of the experimental data to STC considers the impact of varying solar irradiance levels on the temperature of the PV module. The incident irradiance, G_m, determines the short circuit current while both the irradiance and module temperature determine the open circuit voltage, Voc [69].

The Equation (3.1) developed using multiple linear regressions was used to correct the module current and voltage to STC:

$$V_{oc;r} = V_{oc;m} + \alpha(T_r - T_m) + b(G_r - G_m) \tag{3.1}$$

where T_r is the reference temperature, T_m is the measured temperature, $V_{oc,\,r}$ is the module open circuit voltage corrected to STC, $V_{oc;m}$ is the measured open circuit voltage, α - temperature coefficient of the module and b - isolation coefficient ($Vm^2\,W^{-1}$).

$$V = V_m \frac{V_{oc;r}}{V_{oc;m}} \tag{3.2}$$

where V is the module voltage corrected to STC, V_m is the measured module voltage. Values of

current obtained will be normalized using Equation (3.3):

$$I = I_m(\frac{G_r}{G_m}) \tag{3.3}$$

Where I is the current of the module corrected to STC, I_m is the measured module current, G_m is the measured solar irradiance, and G_r is the reference solar irradiance. Average values of normalized voltage and current were obtained. Values of maximum power, P_{max} were calculated by getting the product of current at maximum power and voltage at maximum power. I-V and P-V curves were plotted and analysed using Origin 6.0 software. Values of open circuit voltage, short circuit current and maximum electrical power, P_{max} dissipated by the modules were obtained from the graph using Equation (3.4);

$$P_{max} = I_{mp} \text{ x } V_{mp} \tag{3.4}$$

3.3 Determination of conversion efficiency

Efficiencies η of the PV modules were calculated using Equation (3.5).

$$\eta = \frac{P_{\max}}{A \times G} \times 100\% \tag{3.5}$$

where P_{max} is the maximum power obtained from the I-V curve of the PV module.

A is the area of the PV module. The length and width of the PV module were measured, and its area A was calculated (appendix 1). G is the solar irradiance, which is power per unit area received from the sun and has a standard value of 1000 W/m^2.

The efficiency, η, of the PV modules was then calculated as shown in Appendix 1.

The extracted electrical module conversion efficiencies of the modules and visual inspection results were statistically compared with those of the manufacturer to assess the functionality of the modules.

3.4 Data analysis

FTV200 I-V Tracer and Origin software were used in the analysis of PV module performance. The FTV200 I-V Tracer was employed to extract data of electrical performance parameters, specifically the short-circuit current (Isc), open-circuit voltage (Voc), irradiance and temperature before and after washing of the modules across the four selected schools. The I-V Tracer extracts data at OPC and normalizes it to STC. The formula of efficiency in subsection (3.4) was used to calculate the efficiency of each module after measuring and recording the cross-sectional area, A, of the module. Origin software was then used for graphical analysis.

CHAPTER FOUR: RESULTS AND DISCUSSION

4.0 Introduction

This chapter presents the results obtained from the visual inspection using the International Electrotechnical Commission guidelines, determination of the module maximum power using the current-voltage characterization technique, determination of the efficiencies of the modules and comparison of the module efficiencies with the manufacturer's module efficiency.

4.1 Visual Inspection using the International Electrotechnical Commission (IEC) Guidelines

A checklist for PV modules, as developed by the International Electrotechnical Commission (IEC), Appendix II was used. Visual Inspection results for PV module A installed at Akii Bua Comprehensive Secondary School, Adwari Secondary School, Katine Secondary School and Orungo High School are presented in Table 4.1.

Table 4.1: Visual inspection results for PV module A.

			Defect Present?		
Component	Defect	Schools	No	Yes	Defects Present
1. Label	1.1.Missing	Akii Bua	✓		
		Adwari	✓		
		Katine	✓		
		Orungo	✓		
	1.2.Poorly attached	Akii Bua	✓		
		Adwari	✓		
		Katine	✓		

		Orungo	✓		
	1.3. Information is missing	Akii Bua	✓		
		Adwari	✓		
		Katine	✓		
		Orungo	✓		
	1.4. Incorrect spelling	Akii Bua	✓		
		Adwari	✓		
		Katine	✓		
		Orungo	✓		
2. Back Sheet	2.1.Burn makes	Akii Bua	✓		
		Adwari	✓		
		Katine	✓		
		Orungo	✓		
	2.2.Discolouration	Akii Bua		✓	Discolouration
		Adwari	✓		
		Katine		✓	Discolouration
		Orungo	✓		
3. Junction Box	3.1.Faulty electrical connection	Akii Bua	✓		
		Adwari	✓		

		Katine	✓		
		Orungo	✓		
	3.2.Cracks/breaks/gaps in housing	Akii Bua	✓		
		Adwari	✓		
		Katine	✓		
		Orungo	✓		
	3.3. Sealant Failure	Akii Bua	✓		
		Adwari	✓		
		Katine		✓	Green leakage
		Orungo	✓		
	3.4.Electrical polarity not indicated	Akii Bua	✓		
		Adwari	✓		
		Katine	✓		
		Orungo	✓		
4. Wiring	4.1.Cracks or exposed metal	Akii Bua	✓		
		Adwari	✓		
		Katine	✓		
		Orungo	✓		
5. Frame	5.1.Damaged	Akii Bua	✓		

		Adwari	✓		
		Katine	✓		
		Orungo	✓		
	5.2. Adhesive/sealant failure	Akii Bua	✓		
		Adwari	✓		
		Katine		✓	Adhesive sealant failure
		Orungo	✓		
6. Front Glass	6.1.Cracks	Akii Bua	✓		
		Adwari	✓		
		Katine	✓		
		Orungo	✓		
	6.2.Scratches	Akii Bua	✓		
		Adwari	✓		
		Katine	✓		
		Orungo	✓		
7. Encapsulation	7.1.Discoloration	Akii Bua		✓	Discoloured
		Adwari	✓		
		Katine		✓	Discoloured
		Orungo	✓		

8. Cells	8.2. Snail trails	Akii Bua		✓	Snail trail
		Adwari	✓		
		Katine	✓		
		Orungo	✓		
	8.3. Shiny locally/inconsistent colour	Akii Bua	✓		
		Adwari	✓		
		Katine	✓		
		Orungo	✓		
9. Cell Metallization	9.1.Fingers not connected to the bus bar	Akii Bua	✓		
		Adwari	✓		
		Katine	✓		
		Orungo	✓		
	9.2.Not the same pattern on all cells	Akii Bua	✓		
		Adwari	✓		
		Katine	✓		
		Orungo	✓		
	9.3.Fingers off the edge of the corner of the cells	Akii Bua	✓		
		Adwari	✓		
		Katine	✓		

		Orungo	✓		
10. Cell Interconnection	10.1. Interconnection is discontinuous	Akii Bua	✓		
		Adwari	✓		
		Katine	✓		
		Orungo	✓		
	10.2. Poorly aligned and/or soldered	Akii Bua	✓		
		Adwari	✓		
		Katine	✓		
		Orungo	✓		

A checklist for visual inspection results for modules B installed at Akii Bua Comprehensive Secondary School, Adwari Secondary School, Katine Secondary School and Orungo High School is presented in Table 4.2.

Table 4.2: Visual Inspection results for PV modules B

			Defect Present?		
Component	Defect	Schools	No	Yes	Defects Present
11. Label	11.1. Missing	Akii Bua	✓		
		Adwari	✓		
		Katine	✓		
		Orungo	✓		
	11.2. Poorly attached	Akii Bua	✓		
		Adwari	✓		
		Katine	✓		
		Orungo	✓		
	11.3. Information is missing	Akii Bua	✓		
		Adwari	✓		
		Katine	✓		
		Orungo	✓		
	11.4. Incorrect spelling	Akii Bua	✓		
		Adwari	✓		
		Katine	✓		
		Orungo	✓		

12. Back Sheet	Burn makes	Akii Bua		✓	
		Adwari		✓	Burn marks on diode with rust on cover
		Katine	✓		
		Orungo	✓		
	12.1. Discolouration	Akii Bua		✓	Discolouration
		Adwari	✓		
		Katine		✓	Discolouration
		Orungo	✓		
13. Junction Box	13.1. Faulty electrical connection	Akii Bua	✓		
		Adwari	✓		
		Katine	✓		
		Orungo	✓		
	13.2. Cracks/breaks/gaps in housing	Akii Bua	✓		
		Adwari	✓		
		Katine		✓	Gaps left in the housing
		Orungo	✓		
	13.3. Sealant Failure	Akii Bua	✓		
		Adwari	✓		

		Katine		✓	Sealant failure and green leakage
		Orungo	✓		
	13.4. Electrical polarity not indicated	Akii Bua	✓		
		Adwari	✓		
		Katine	✓		
		Orungo	✓		
14. Wiring	14.1. Cracks or exposed metal	Akii Bua	✓		
		Adwari		✓	Cracks on metal
		Katine		✓	Cracks
		Orungo	✓		
15. Frame	15.1. Damaged	Akii Bua	✓		
		Adwari		✓	Black spot
		Katine	✓		
		Orungo	✓		
	15.2. Adhesive/sealant failure	Akii Bua	✓		
		Adwari	✓		
		Katine		✓	Adhesive sealant failure
		Orungo	✓		

16. Front Glass	16.1. Cracks	Akii Bua		✓	Cracks
		Adwari	✓		
		Katine		✓	Cracks
		Orungo	✓		
	16.2. Scratches	Akii Bua	✓		
		Adwari		✓	Scratches
		Orungo	✓		
		Katine	✓		
17. Encapsulation	17.1. Discoloration	Akii Bua		✓	Discoloured
		Adwari		✓	Discoloured
		Katine	✓		
		Orungo	✓		
18. Cells	18.1. Snail trails	Akii Bua	✓		
		Adwari	✓		
		Katine	✓		
		Orungo	✓		
	8.3. Shiny locally/inconsistent colour	Akii Bua	✓		
		Adwari	✓		
		Katine	✓		

		Orungo	✓		
19. Cell Metallization	19.1. Fingers not connected to bus bar	Akii Bua	✓		
		Adwari	✓		
		Katine		✓	Disconnected fingers
		Orungo	✓		
	19.2. Not the same pattern on all cells	Akii Bua	✓		
		Adwari	✓		
		Katine	✓		
		Orungo	✓		
	19.3. Fingers off the edge of corner of the cells	Akii Bua	✓		
		Adwari	✓		
		Katine		✓	Fingers off at the corner of a cell
		Orungo	✓		
20. Cell Interconnection	20.1. Interconnection is discontinuous	Akii Bua	✓		
		Adwari	✓		
		Katine	✓		
		Orungo	✓		
		Akii Bua	✓		

	20.2. Poorly aligned and/or soldered	Adwari	✓		
		Katine	✓		
		Orungo	✓		

4.1.1 Inspection results of the PV modules at Orungo High School

Visual inspection for module A at Orungo High School is presented in Table 4.1. Module A had dust and debris accumulated on it. Discolouration was present on the cell encapsulation of the module at Orungo High School. Accumulation of dust and debris results in shading of the modules, hence affecting the maximum power output of the module. Visual inspection results for module B at Orungo High School, presented in Table 4.2, showed no physical defect except the presence of Bird droppings, as in Figure 4.1, with a lot of dust and debris accumulated.

Figure 4.1: Bird dropping on the module B Orungo SS.

Accumulation of dust and debris results in physical shading of the module, and this affects the functionality of the module [70].

4.1.2 Visual Inspection of the PV modules at Adwari SS

Visual inspection results for module A at Adwari Secondary School, presented in Table 4.1, revealed that module A had a snail trail with dust accumulated and scratches on its surface. The

presence of these factors reduces light transmission and creates localized hotspots. These hotspots lead to energy loss and may affect the overall module efficiency. While visual inspection results for module B at Adwari Secondary School, presented in Table 4.2, indicate that the back sheet of module B at Adwari Secondary School had burn marks as shown in Figure 4.2.

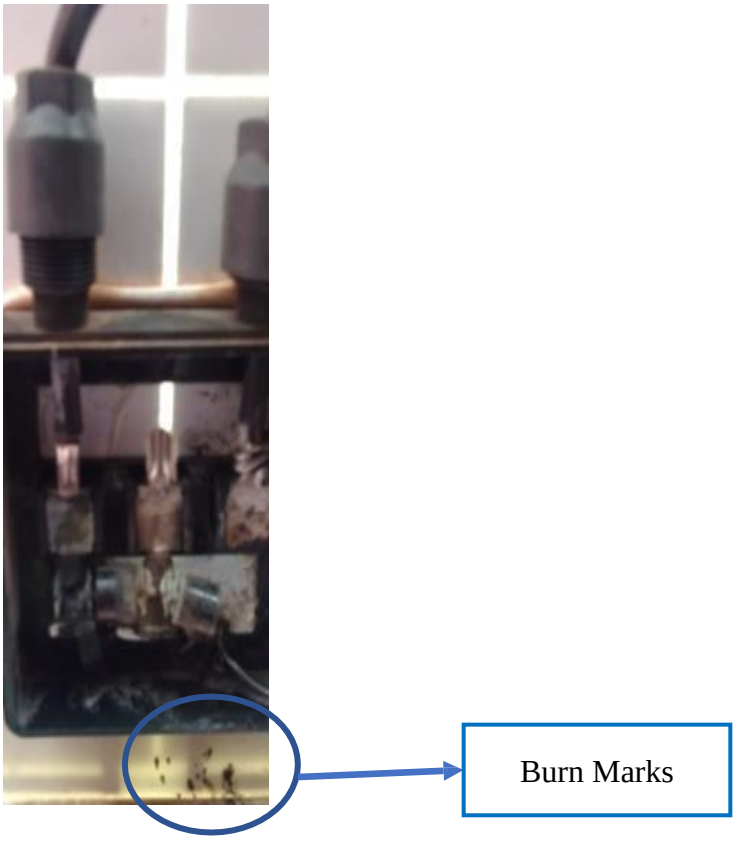

Figure 4.2: A short-circuited diode at Adwari Secondary School.

The burn marks could be due to electrical faults within the solar module that could have resulted in abnormal levels of current flow, causing localized heating (hotspots) [46], blackened spots, and snail trails as observed in Figure 4.3 and excessive heat built up in the solar module due to environmental factors like high temperatures or inadequate heat dissipation.

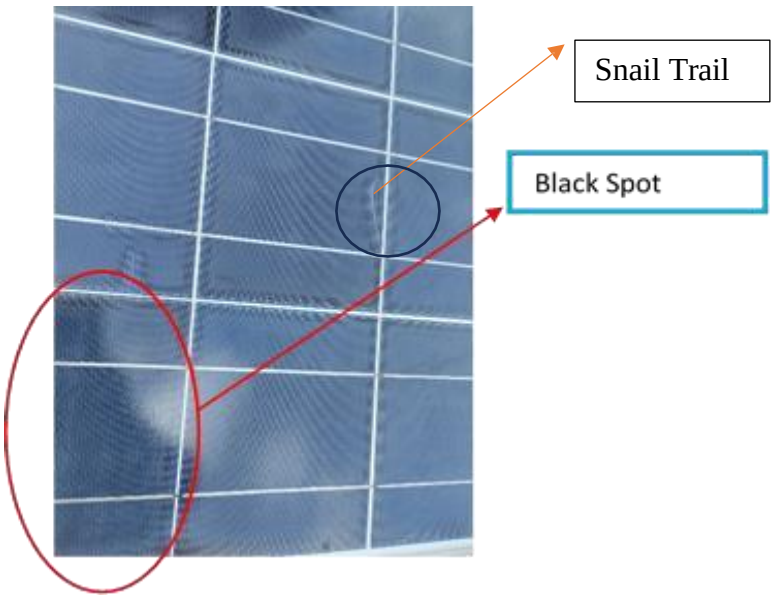

Figure 4.3: Module at Adwari SS with a black spot and snail trail.

It is important to note that burn marks on the back sheet of a solar module remain a typical sign of damage or malfunction and degradation [70], which should always be inspected and resolved promptly for optimal performance and safety [71]. The back sheets and the encapsulant of PV modules are not perfectly air-tight and are therefore susceptible to diffusion of gases and moisture [72]. Figure 4.4 at Adwari Secondary School shows modules A and B with lines of water ingression.

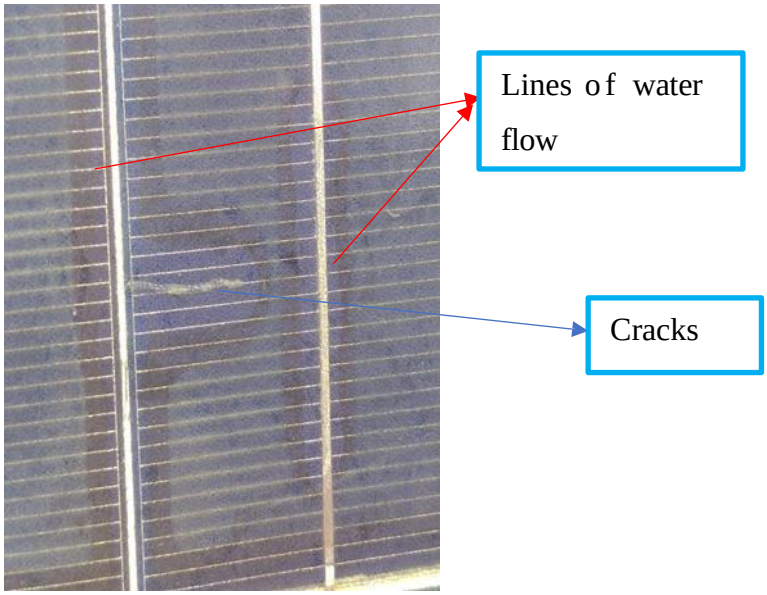

Figure 4.4: Cracks and water ingression on the module at Adwari Secondary School.

This particular finding is in line with the literature review in section 2.4 (Module faults and failures). Climatic conditions of the place, the age of the modules, and the materials or the module technology used could be other factors to consider [73]. Figure 4.4 shows moisture ingress with discolourisation, lines of water flow, cracks, and scratches, all of which negatively impact the functionality of the modules. Discoloration on encapsulants can lead to lower energy output due to reduced light transmission. It may cause localized hotspots on the module surface, which can further impair performance and potentially damage the module. The diode cover in Figure 4.5 at Adwari SS was filled with brownish powdered rust or corroded materials, probably produced due to overheating.

Figure 4.5: Diode cover corroded at Adwari Secondary School.

In a solar cell circuit, the diode is typically connected in a reverse bias configuration to prevent any reverse current flow. It can act as a protection mechanism, blocking the current from flowing back into the solar cell when it is not receiving sunlight. When the diode becomes destroyed, as shown in Figure 4.5, it becomes an open circuit with no current flowing through the diode or the solar cell. This could be the reason why module B did not give any power output.

4.1.3 Visual Inspection of PV modules at Akii Bua Comprehensive Secondary School

Visual inspection results at Akii Bua Comprehensive Secondary School showed similar defects in both module A and B, as indicated in both Table 4.1 and 4.2. Results carried out on PV modules installed at Akii Bua Comprehensive Secondary School revealed that no maintenance schedules for the PV modules were done. This is evidenced by Figure 4.6, where birds have built their nests under both modules [74], and a very thick layer of dust existed on the modules, bird droppings

and other debris on both modules, resulting in energy yield loss [75].

Figure 4.6: Bird's nest under the modules at Akii Bua Comprehensive Secondary School.

The nests and debris can act as an insulating layer [76], trapping heat under the PV module. This heat buildup can increase the operating temperature of the solar cells, reducing their efficiency and potentially causing damage over time [77]. Nests and other materials can also introduce additional weight and pressure on the solar module, potentially leading to damage to the diodes or other components within the module. Damage to the diodes can disrupt the flow of electricity and negatively impact the overall power generation of the module [78].

In some cases, the bird's nest and accumulation of dry organic substances can cause fire hazards to the module, especially if the modules are made of flammable materials [78]. This can increase the risk of fire, which can damage the diodes and other components, leading to a complete loss of power generation. At Akii Bua Comprehensive Secondary School, the modules are shaded as early as 10:00 am. This is because big trees surrounded the house where the modules are installed. This phenomenon results in variations in the amount of irradiance, hence creating an instant reduction in the values of I_{SC} and V_{OC}.

4.1.4 Visual Inspection of PV modules at Katine SS

Visual inspection results for modules A and B at Katine Secondary School have been presented in Table 4.1 and Table 4.2. A module at Katine Secondary School with a hot spot and Snail trails is

shown in Figure 4.7.

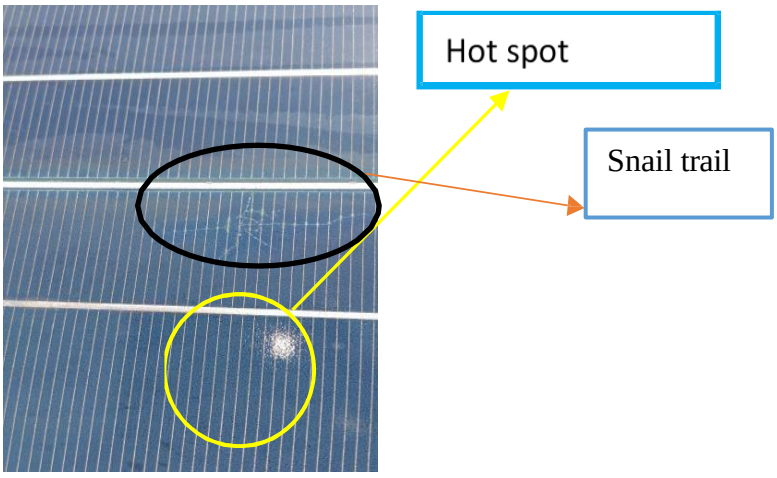

Figure 4.7: Module with hot spot and snail trail at Katine SS.

A module at Katine Secondary School in Figure 4.8 with broken sealant, Lines of water flow and brown colouration.

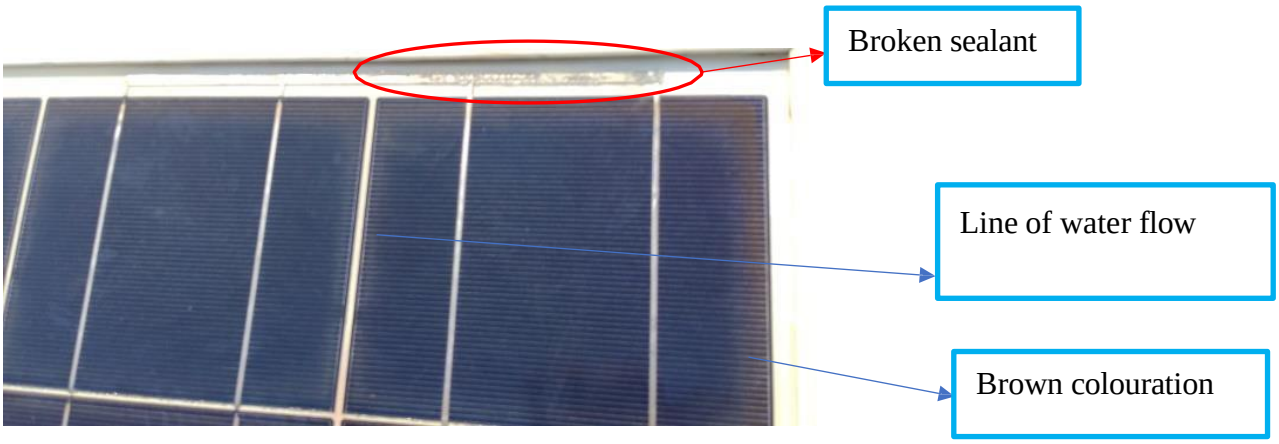

Figure 4.8: A Module with sealant failure at Katine Secondary School.

At Katine Secondary School, Sealant Failures were observed on the modules as shown in Figure 4.8. This could be due to mechanical stress like wind loads or thermal expansion, moisture ingress, and

contraction, since these modules are installed in a very hot part of Northern and Eastern Uganda. It could also be due to the manufacturing defects, like improper mixing of the sealant components or inconsistencies in the sealing process. Gaps were left at the metal sealant, which, over a period of time, caused water ingression, leading to short circuiting of the cells, hence leakage of the greenish substances on the modules installed at Katine Secondary School, Eastern Uganda, as in Figure 4.9.

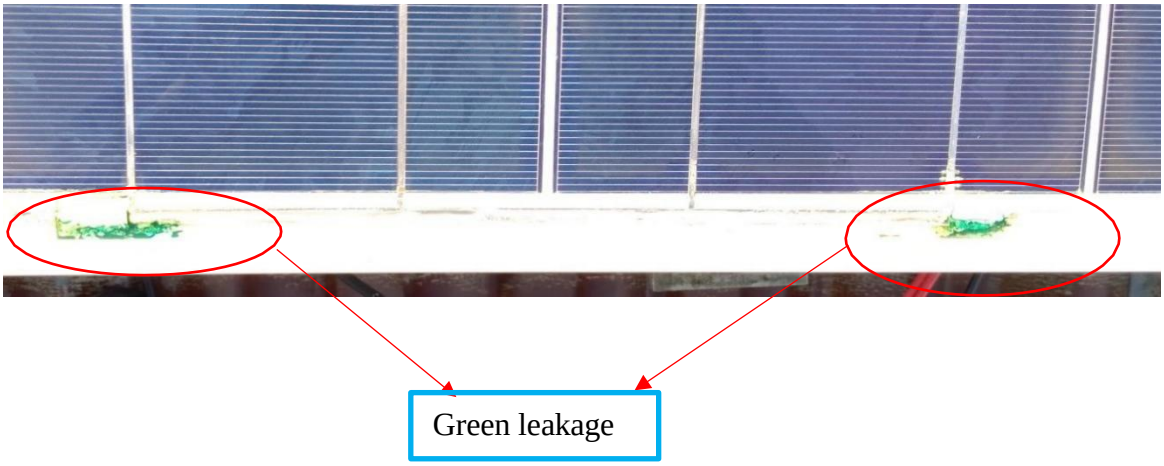

Figure 4.9: Module with greenish leakage at Katine Secondary School.

Water contains minerals and impurities that can lead to corrosion of the metal components in the solar module. This can affect the electrical connections and structural integrity of the module, leading to decreased performance and potential failures. If there is a difference in electrical potential between the solar cell and the frame of the module, it can result in a green leakage as shown in Figure 4.9 [67]. This green leakage is usually brought about by potential induced degradation (PID), which occurs when there is an electrical potential difference between the solar cell and other conductive elements, according to [79], within the module. A high level of moisture exacerbates the effects of PID [80] [81]. When water infiltrates the module, it can carry ions that enhance the leakage current, leading to increased green leakage [82]. The green leakage forms an unintended electrical pathway, diverting current away from the intended circuitry, which leads to power loss, reducing the overall efficiency of the solar module. Several factors can lead to significant degradation between the solar cells and the PV module frame due to electrochemical

interactions [83]. Moisture ingress in PV modules is also the leading cause of encapsulant failures, as it can cause delamination and metal discolourisation [84]. In a solar PV system, multiple solar modules are connected in series or parallel [85] to generate electricity. Each solar module consists of multiple interconnected solar cells. These solar cells may have slight variations in their electrical characteristics, such as their current output. When solar modules with different current outputs are connected together, it can result in a current mismatch. This means that the total current produced by the solar modules is limited to the current of the weakest module or the module with the lowest current output [86]. This is because the component with the lowest resistance constrains the current flow in a series circuit. Current mismatch in a solar PV system can lead to a decrease in the overall system's efficiency and power output. It can also cause a phenomenon known as "hotspot," where excessive heat is generated in the weaker solar module due to the mismatched current flow which is clearly shown in Figure 4.7. This can potentially damage the module or reduce its efficiency and lifespan. The encapsulation of both modules was discoloured brown with cracks on the modules and some fingers disconnected especially on module B. This would account for the lower values of I_{SC} and V_{OC} of module B as evidenced in Table 4.3. Most of the modules installed at Katine SS were also abandoned on the roof with most of the accessories not functional.

4.2 Determination of the Module Maximum power using the current-voltage characterization technique

In order to determine the maximum power of the modules, I-V curves were extracted using the I-V tracer.

4.2.1 PV module I-V curves

The PV module I-V curves are presented in Figures 4.10, 4.11, and 4.12. In the Figures, A stands for module A before washing, and Aw stands for module A after washing.

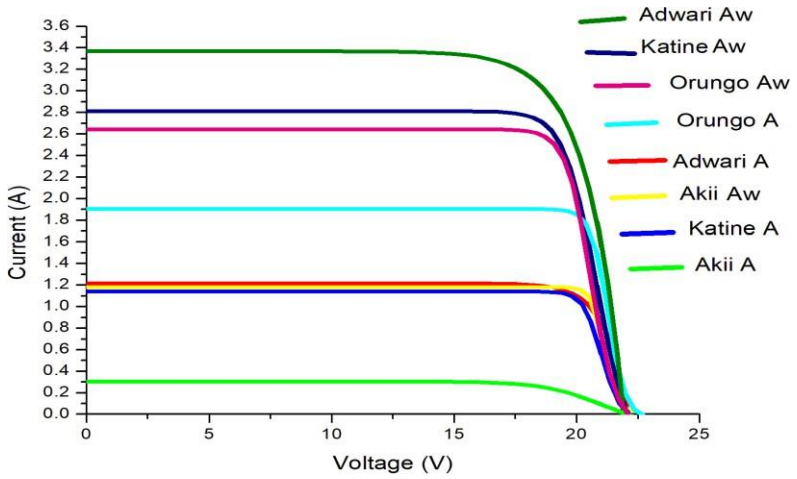

Figure 4.10: I-V curves for module A.

As discussed in Chapter 2, subsection 2.3.1, short circuit current depends linearly on light intensity [16]. In contrast, open circuit voltage depends on saturation current, as also discussed in subsections 2.2.1 and 2.2.2 of the literature review. Therefore, data from Figure 4.10 shows that washing generally improves the performance of PV modules, as revealed by variations in short-circuit current (I_S) and open-circuit voltage (V_{OC}).

The study revealed that, at Katine SS, module A I_{SC} before and after washing remained constant at very low values of 2.24 A as well as its V_{OC} 19.07 V. The low but constant values of I_{SC} and V_{OC} for Module A could have been attributed to several factors, including temperature [87], bypass diode failures, hotspots, and shaded cells [88]. Bypass diodes prevent excessive voltage drop across shaded or faulty cells and allow current to bypass shaded or defective cells, preventing significant drops in

overall current while maintaining overall V_{oc}. Due to solder fatigue [89], V_{OC} may also decrease slightly due to aging and remain within acceptable limits. Modules at Orungo HS showed the highest increase in I_{SC} and $V_{OC}$for both modules (A I_{SC} 4.51 A, Aw I_{SC} 5.54 A) and (A V_{OC}, 19.64 V and Aw V_{OC} 20.21 V). Adwari SS demonstrated an increase in I_{SC} from A I_{SC}: 3.41 A to Aw I_{SC}: 3.73 A with no change in V_{OC} 19.64 V, indicating some performance enhancement after washing the module. This slight increase in I_{SC} indicates defects on the module. Module A at Adwari SS had snail trails, cracks, a hotspot as shown in Figure 4.7, and dust accumulation. Its bypass diodes allowed current to bypass shaded or defective cells, preventing significant drops in the overall current [90].

However, the PV module at Akii Bua Comprehensive School exhibited a decrease in I_{SC} for module A from 3.49 A before washing to 0.60 A after washing, with a reduction in V_{OC} from 19.36 V to 18.78 V.

The I-V curves for module B in the four selected schools are shown in Figure 4.11. B stands for module B before washing, and Bw stands for module B after washing.

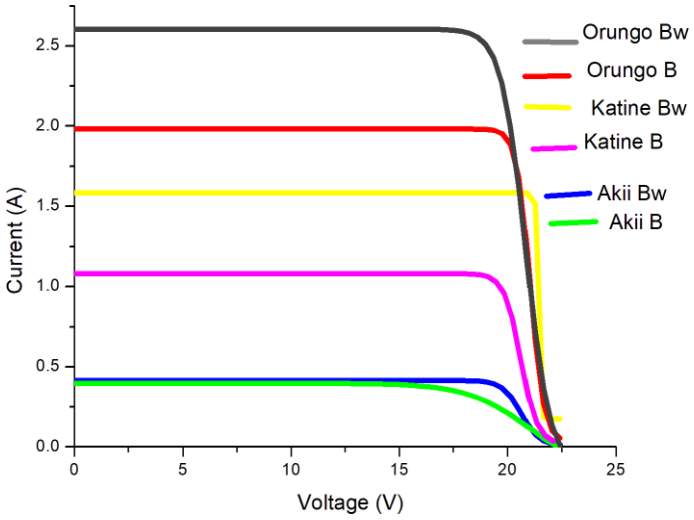

Figure 4.11: I-V curves for module B.

From Figure 4.11, Katine Secondary School module B I_{SC} increased significantly from 2.63 A before washing to 3.0 A after washing, module B at Katine Secondary School before washing, gave the lowest V_{OC} because its modules had soiling, cracks and breakage [89], a lot of water ingress which caused Light-Induced Degradation (LID) [89] and Potential-Induced Degradation (PID) [69]

evidenced by the green leakage and general delamination and discoloration [89] of the metal casing with sealant failures and corrosion [89] according to visual inspection results for module A and B at Katine Secondary School presented in Table 4.1 and Table 4.2. However, after washing, its V_{OC} value increased from 18.74 V to 19.80 V. This could be due to the removal of the dust and debris that had shaded the module from maximum irradiance. Module B at Orungo HS showed the highest increase in I_{SC} and V_{OC} (BI_{SC} 4.52 A, Bw, I_S , 5.20 A) and (B V_{OC} 19.64 V, Bw V_{OC} 19.36 V), indicating improved performance post-washing. At Akii Bua Comprehensive Secondary School, module B showed slight improvements in I_{SC} (Bw I_{SC} 0.57 A) with a lower V_{OC} of 18.78 V since its modules were covered with thick dust, birds had built their nests under it, causing overheating under the modules. Further findings revealed that the PV modules installed at Akii Bua Comprehensive Secondary School are typically always shaded before midday, resulting in variations in the amount of irradiance, hence creating an instant reduction in the values of I_{SC} and V_{OC}. Adwari Secondary School, however, had burn marks at its back, diode failures evidenced by rusts formed on the diode cover as shown in Figure 4.5. The module had a black spot, which indicated failure in the normal functioning of the cells. Module B, therefore, did not indicate any measurement of both short circuit current and open circuit voltage. Figure 4.12 shows the I-V curves for string AB in the four selected schools. AB stands for string AB before washing, and ABw stands for string AB after washing.

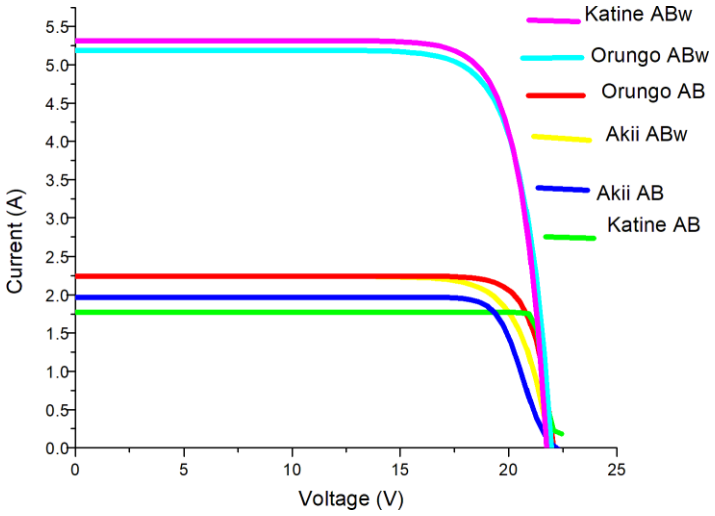

Figure 4.12: I-V curves for strings AB.

Katine Secondary School string AB showed a slight increase in I_{SC} from 5.37 A before washing to 5.39 A after washing, with an increase in V_{OC} from 18.79 V before washing to 20.70 V after washing. Akii Bua Comprehensive SS Bw I_{SC}0.60 A) and V_{OC} (BV_{OC} 18.78 V, BwV_{OC} 19.36V) string had a constant short circuit current with an increase in the open circuit voltage after washing from 19.08 V to 19.92 V. Table 4.3 is the summary of the I_{SC} and V_{OC} of each module in a school before and after washing.

4.2.2 Power – Voltage Curves

The power obtained from the I-V curves was plotted against module voltages as shown in Figures 4.13, 4.14 and 4.15. The maximum power was then extracted from the PV curves.

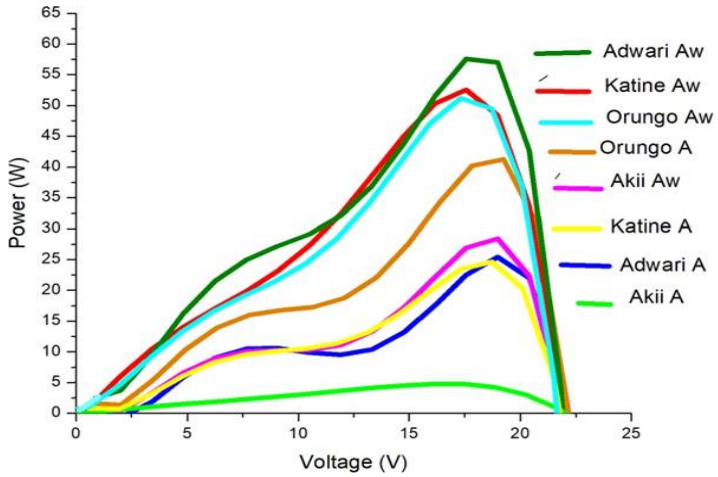

Figure 4.13: P-V curves for module A in the selected schools.

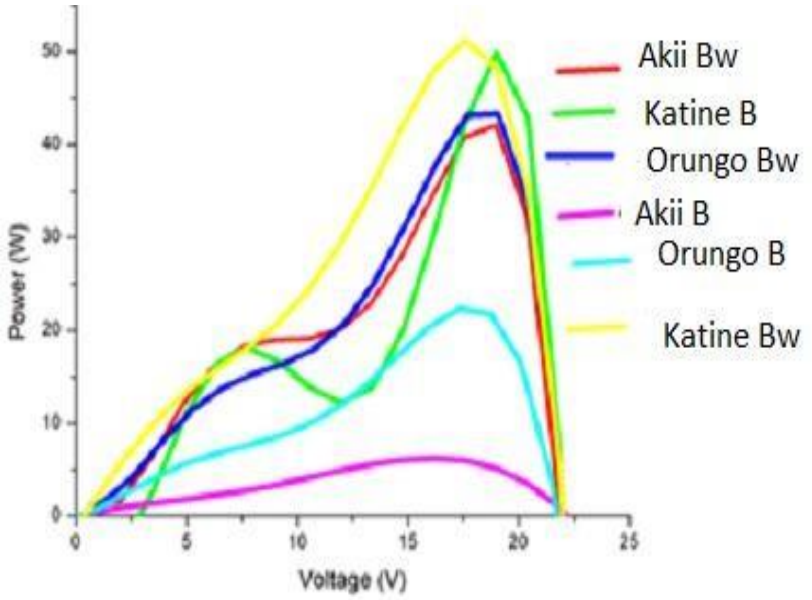

Figure 4.14: P-V curves for module B.

The P-V curves for strings AB in the selected secondary schools. AB are strings before washing, and ABw are strings after washing Figure 4.15.

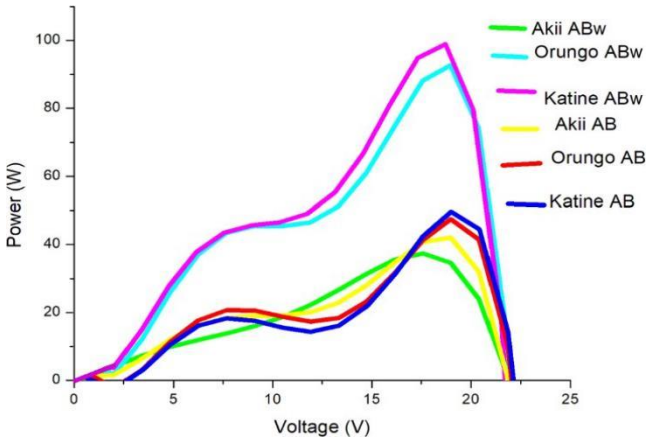

Figure 4.15: P-V curves for strings AB.

The summary of maximum power, irradiance, and temperatures of the PV modules before and after washing is shown in Table 4.4.

Table 4.3: A Summary of P_{max}, irradiance, and temperature for the PV modules before and after washing

School	Pmax/Irradiance	Module A	Module B	String AB	Module Aw	Module Bw	String ABw
Orungo High School	Pmax	37.49	35.82	39.77	57.52	54.51	61.88
	Irradiance	1101.4	1076.33	1089.60	1270	1269.45	795.57
	Temp	25.00	38.92	39.74	31.13	35.96	32.35
Katine SS	Pmax	21.84	8.64	22.37	34.60	20.80	40.04
	Irradiance	761.07	708.38	685.06	1099.76	1112.07	608.44
	Temp	34.19	35.42	35.19	34.35	33.89	31.64
Akii Bua Comp Sch	Pmax	4.60	5.73	34.71	18.74	5.86	34.71
	Irradiance	933.97	979.94	959.21	933.97	1070.91	1077.23
	Temp	36.85	38.72	38.72	36.09	32.89	33.59
Adwari SS	Pmax	35.84	-	-	36.10	-	36.71
	Irradiance	933.97	-	-	1025.69	-	-
	Temp	32.28	-	-	34.40	-	-

The maximum power obtained was analysed as shown in Figures 4.16, 4.17 and 4.18.

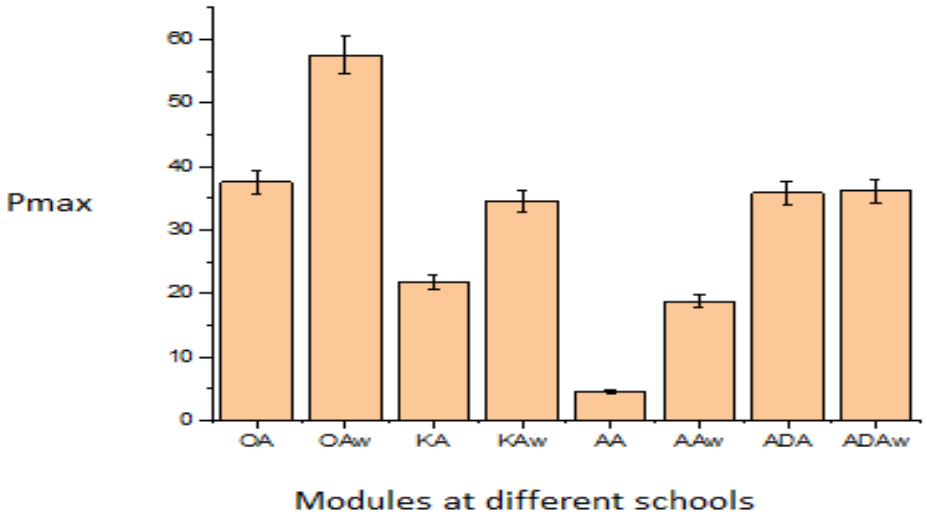

Figure 4.16: Maximum power of modules A before and after washing.

In Figure 4.16, OA represents Orungo High School module A before washing, OA_w after washing, KA represents Katine SS module A before washing, KAw after washing, AKA represents Akii Bua Comprehensive SS module A before washing, AKA_w after washing, and ADA represents Adwari SS module A before washing and ADA_w after washing.

The results revealed that washing the modules increases the module power output. This is because some physical particles which had accumulated on the modules were washed away by water, hence more irradiance could reach the module cells and generate power. The increment was more pronounced at module A installed at Akii Bua Comprehensive SS (73.7%), followed by Katine S.S (37.1%), Orungo High School (34.8%), and Adwari S.S (1.4%).

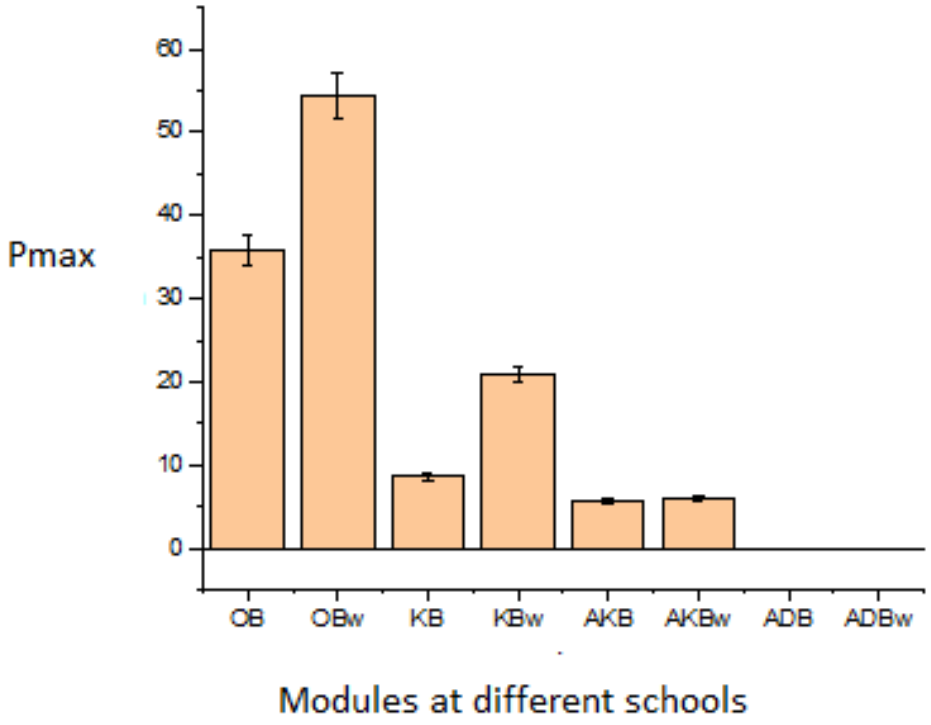

Figure 4.17: Module B of different schools.

In Figure 4.17, OB represents Orungo High School module B before washing, OB_w after washing, KB represents Katine SS module B before washing, KB_w after washing, AKB represents Akii Bua Comprehensive SS module B before washing, AKB_w after washing, and ADB represents Adwari SS module B before washing and ADB_w after washing.

The results indicated that washing the modules increases the module power output. The increment was more pronounced at Katine SS (57.1%), followed by Orungo High School (33.3%), Akii Bua Comprehensive SS (5.9%), while module B at Adwari SS didn't give any power output. The inability to generate power by module B at Adwari SS could be attributed to the current limiting features like cracks, black spots, diode failure, and snail trails, which were detected on the module by visual inspection.

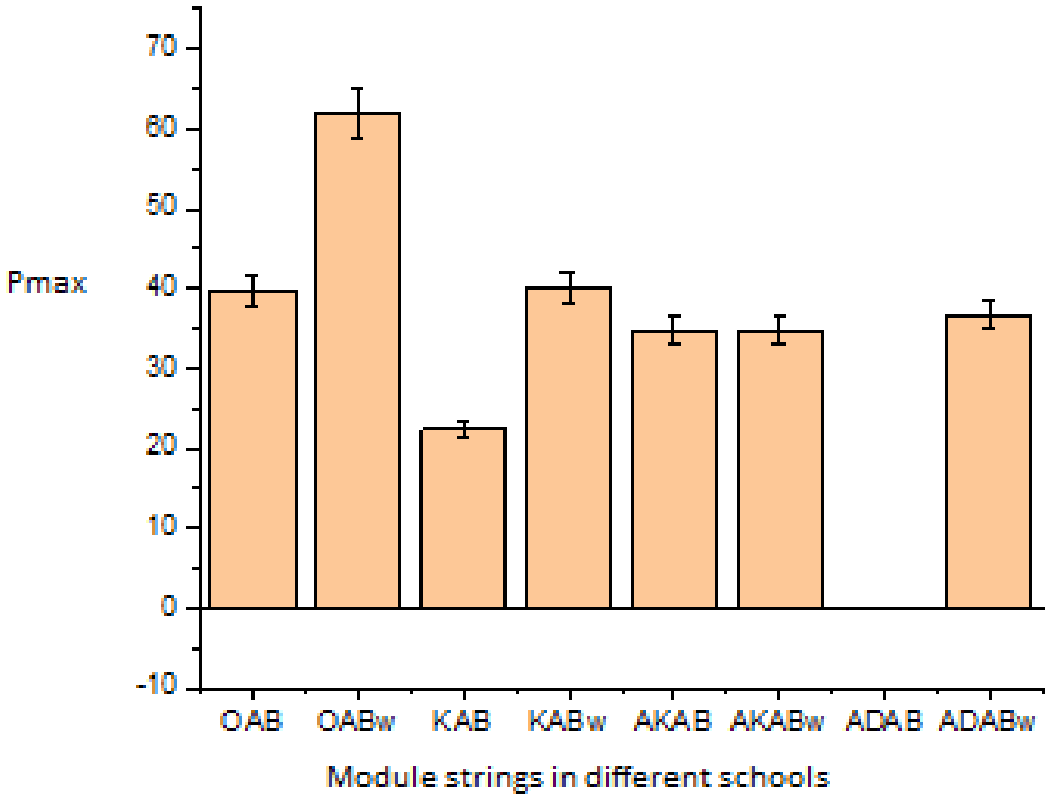

Figure 4.18: Maximum power of the module strings AB before and after washing.

In Figure 4.18, OAB represents Orungo High School module string AB before washing, OAB_w after washing, KAB represents Katine SS module string AB before washing, KAB_w after washing, AKAB represents Akii Bua Comprehensive SS module string AB before washing, $AKAB_w$ after washing and ADAB represents Adwari SS module string AB before washing and $ADAB_w$ after washing.

The results showed that, for Orungo High School and Katine SS, washing the modules increases the module power output. The increment was more pronounced at Katine S.S (43.8%) than at Orungo S.S (36%). However, there was no increment in power output at Akii Bua Comprehensive SS, while the module string at Adwari SS could only give power after washing.

4.3 Determination of Conversion Efficiencies of the modules

The efficiencies of the PV modules were calculated as indicated in Appendix 1, and the results tabulated as shown in Table 4.4.

Table 4.4: Efficiencies of Modules and Strings at the different schools

School	**A**	**B**	**AB**	**A_w**	**B_w**	**AB_w**
Orungo High School	4.62	4.41	4.90	7.09	6.71	7.62
Katine SS	2.69	1.06	2.76	4.24	2.57	4.93
Akii Bua Comp. SS	0.69	0.72	2.4	2.30	0.84	4.28
Adwari SSS	4.41	-	-	4.66	-	-

The efficiencies were analysed as shown in Figures 4.19, 4.20, and 4.21.

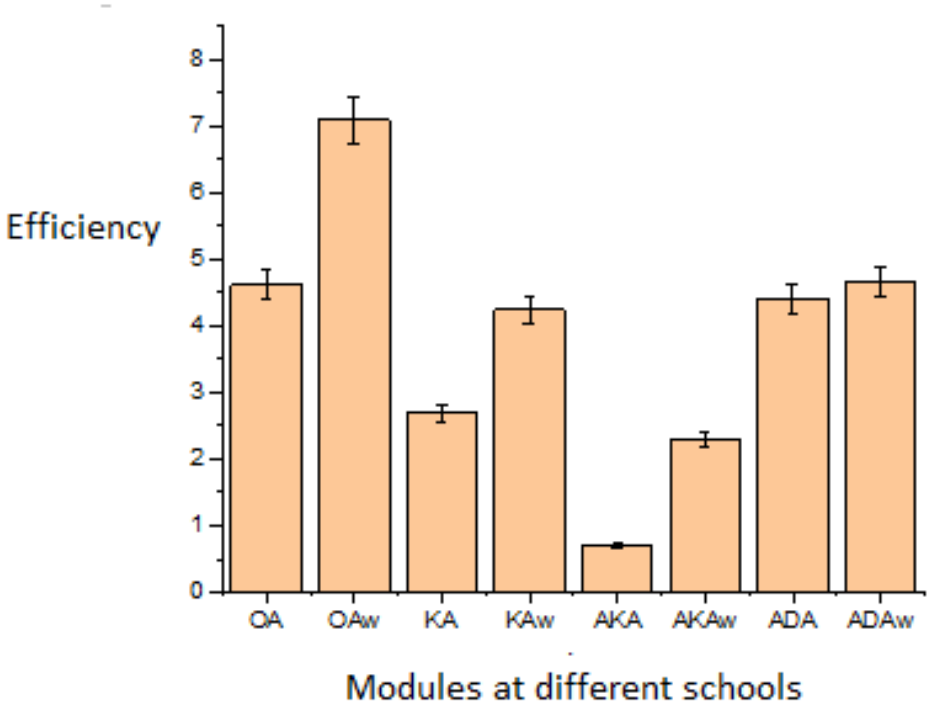

Figure 4.19: Comparison of efficiencies of modules A.

According to Figure 4.19, the efficiency of module A at Orungo High School, Katine S.S, Akii Bua

Comprehensive SS, and Adwari SS increased by 2.5%,1.6%, 1.6% and 0.2% respectively, after washing. This implies that washing has the effect of removing dust and other particles responsible for shading the modules. When the modules are shaded, the power output and hence the efficiency are reduced. Shading was more pronounced on the modules at Orungo High School and least pronounced on the modules at Adwari S.S.

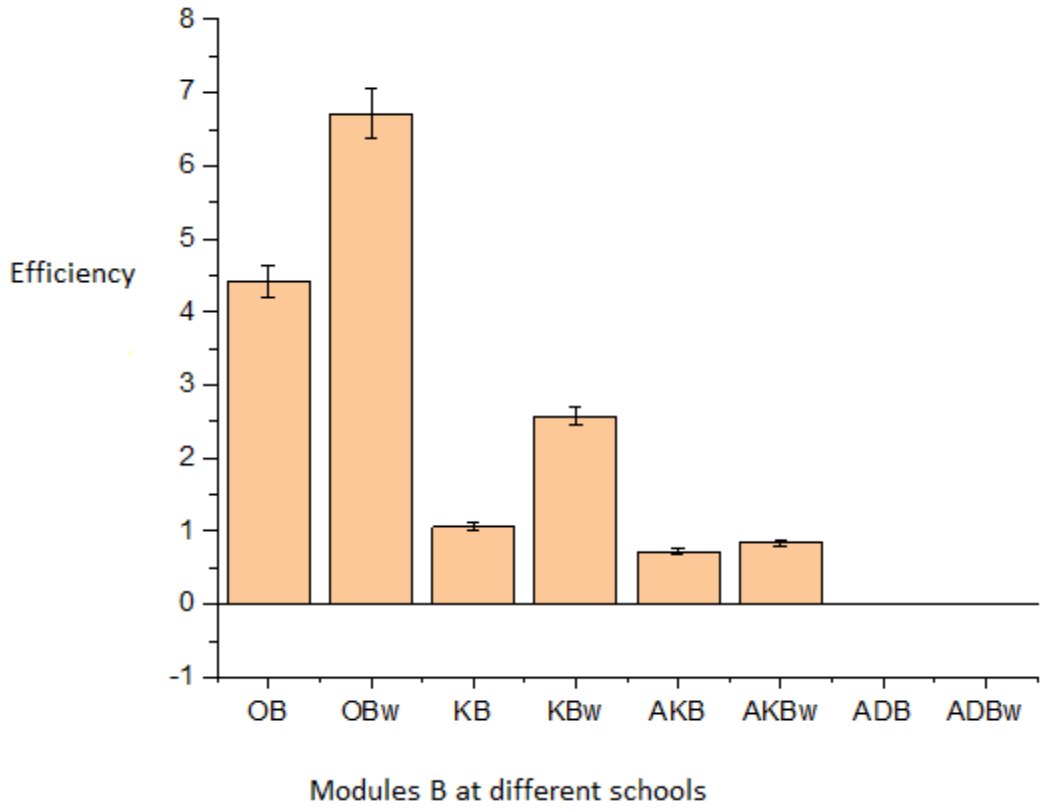

Figure 4.20: Comparison of efficiencies of module B.

According to Figure 4.20, the efficiency of module B at Orungo High School, Katine SS and Akii Bua Comprehensive SS increased by 2.3%,1.5% and 0.2% respectively, after washing. These variations in efficiencies indicate that shading was more pronounced on the modules at Orungo High School and least pronounced on the modules at Akii Bua Comprehensive SS. As seen in Figure 4.2, module B at Adwari SS did not give any power output, and this suggests why the efficiency is 0 %.

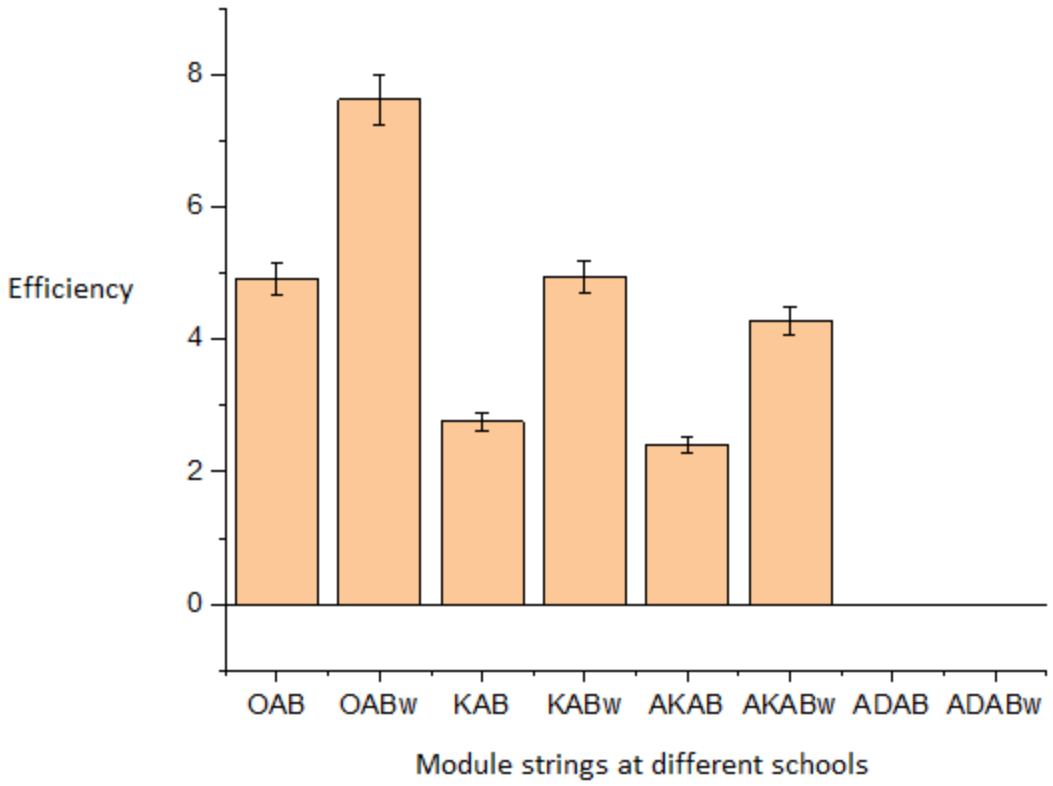

Figure 4.21: Comparison of efficiencies of module strings AB.

According to Figure 4.21, the efficiency of module string AB at Orungo High School, Katine SS and Akii Bua Comprehensive SS increased by 2.8 %,2.2 % and 1.9 % respectively, after washing. These variations in efficiencies indicate that shading was more pronounced on the module string at Orungo High School and least pronounced on the module string at Akii Bua Comprehensive SS. Since module B at Adwari S.S. seems to be faulty, as seen from Figure 4.20, putting it in a string with a functioning module would make it have an adverse effect on the module string performance since the weakest module determines the string output. This explains why the efficiency of the module string at Adwari SS is 0 %.

4.3.1 Comparison of the module efficiencies with those of the manufacturer

The manufacturer's module efficiency of 13.6 % was computed from the nameplate information and is shown in Appendix III. The manufacturer's module efficiencies at the time of manufacture and after degradation were considered for comparison. The degradation rate of polycrystalline PV modules is 1% per year [19]. The determined module efficiencies after washing were the ones used

for comparison in this study.

Efficiencies for modules A for Orungo High School, Katine S.S, Akii Bua Comprehensive SS, and Adwari S.S were 7.09 %, 4.24 %, 2.30 % and 4.66 % respectively. The module efficiency drop from that of the manufacturer was 6.5 %, 9.4 %, 11.3 % and 8.9 % for Orungo High School, Katine S.S, Akii Bua Comprehensive SS, and Adwari SS, respectively. Since this module was installed 10 years ago, the efficiency at the time of this study is expected to drop by 10%, hence reducing the manufacturer's module efficiency from 13.6% to 12.2%. Therefore, the actual module efficiency drop from that of the manufacturer would be 5.1 %, 8.0 %, 9.9 % and 7.5 %. For Orungo High School, Katine SS, Akii Bua Comprehensive SS and Adwari SS, respectively. These results indicate that module A at Orungo High School comparatively performed better, followed by module A at Adwari SS, module A at Katine SS and module A at Akii Bua Comprehensive SS.

Efficiencies for modules B for Orungo High School, Katine SS, Akii Bua Comprehensive SS, and Adwari SS were 6.7 %, 2.6 %, 0.8 % and 0 % respectively. The module efficiency drops from that of the manufacturer were 6.9 %, 11 %, 12.8 % and 13.6 %. For Orungo High School, Katine SS, Akii Bua Comprehensive SS and Adwari SS, respectively. Since the manufacturer's module efficiency reduces to 12.2% due to degradation, the actual module efficiency drop from that of the manufacturer would be 5.5 %, 9.6 %, 11.4 % and 12.2 %. For Orungo High School, Katine SS, Akii Bua Comprehensive SS, and Adwari SS, respectively. These results indicate that module B at Orungo High School comparatively performed better, followed by Module B at Katine SS, module B at Akii Bua Comprehensive SS and module B at Adwari S.S. From these results, it is clear that module A in all the schools performed better than module B.

CHAPTER FIVE: CONCLUSIONS AND RECOMMENDATIONS

5.0 Introduction

This chapter presents the conclusions and recommendations arrived at in this research.

5.1. Conclusion

The study comprehensively evaluated the performance of roof-mounted photovoltaic (PV) modules in rural secondary schools in Northern and Eastern Uganda. Visual inspection and electrical characterization were successfully performed on the modules.

During visual inspection, several current-limiting features were identified on the modules, and these include green leakage, water ingress, discolouration, cracks, snail trails, scratches, black spots, dust, debris, bird droppings, bird nests, burnt spots on diodes, rust, broken sealant, and broken cell interconnects. Modules at Akii Bua Comprehensive SS were always shaded by trees as early as 10:00 am.

At a degradation rate of 1% per annum for polycrystalline PV modules [19], the modules were found to have degraded in efficiency from 13.6% to 12.2% over a period of 10 years. The electrical characterization results revealed that the maximum power output of the PV modules was higher after washing the modules. The modules at Orungo High School produced the highest power (62 W), while the modules at Akii Bua Comprehensive School produced the lowest (34.5 W). The drop in module efficiencies as compared to the manufacturer's efficiency with degradation taken into account was found to be highest for the modules at Akii Bua Comprehensive School (11.3%) and lowest for the modules at Orungo High School (5.5%).

5.2. Recommendations

The MoES should recruit technicians for routine maintenance and monitoring of PV modules and accessories in the pilot rural secondary schools.

Electroluminescence imaging (EL) and large area lights beam induced current measurement (LALBIC) technique should be carried out on those modules to establish current-limiting features that are not visible to the human eye.

Similar studies should be done in Central and Western Uganda.

REFERENCES

1. Rudenauer, S.H., *The Ugandan energy sector - Renewables' enormous potential is yet to deliver*.
2. Richard, K., *Uganda 100% Renewable Energy Scenario and plan 2050. A journal published by Uganda Coalition for Sustainable Development (UCSD)*.
3. Bank, W., *Energy for Rural Transformation Project.* 2014.
4. Farrell, G., *Survey of ICT and education in Africa. Uganda country report*. 2007.
5. Deep, A., *Assessing Roof Suitability for Solar Panel Installation. Illumine i*.
6. Patthy, G.B., Z. Závodi-Fodor, and M. Jakab, *Assessing the Feasibility of Integrating a Thermal Separational Method with PV Recycling Technologies.* Thermo, 2025. **5**(1): p. 10.
7. Marsh, J., *How do solar cells work? Photovoltaic cells explained*. Energy Sage.
8. Sinha, A., *Glass/glass photovoltaic module reliability and degradation: a review.* Journal of Physics D: Applied Physics, 2021. **54**(41).
9. Buerhop-Lutz, C., *PV modules and their backsheets-A case study of a Multi-MW PV power station.* Solar Energy Materials and Solar Cells, 2021. **231**.
10. Maes, A., *Overview of encapsulant materials in photovoltaic modules.* Sandia National Laboratories, 2019.
11. Tummalieh, A. and A.J.B. Christian Reichel, *Holistic design optimization on the PV module frame: CTM, FEM, COO and LCA analysis*. 2021.
12. Kalejs, J., *Junction box wiring and connector durability issues in photovoltaic modules.* Proceedings of SPIE - The International Society for Optical Engineering, 2014. **9179**.
13. Chaaban, M.A., *PV Module Performance Characteristics. AE 868 Commercial solar electric systems 2023*.
14. Sheikh, A., *Understanding PV Module Performance Characteristics*. 2024: EE Power.
15. Rezk, H.e.a., *Performance of data acquisition system for monitoring PV system parameters, Measurement, 2017. 104: p. 204-211.* 2017.
16. G. Bunea, W., K., Meydbray, Y., campbell,M., and Ceuster, D.D.,, *Low light pefornance of mono- crystalline silicon cells. 4th world conference on photovoltiac energy conference, Waikoloa, HI, pp. 1312-1314, 2006.* 2006.
17. Van Sark, W.G.J.E., *Teaching the relation between solar cell efficiency and annual energy yield.* 2007. **28**.
18. Lorenzo, E., *Solar electricity: engineering of photovoltaic systems*. 1994: Earthscan/James & James.
19. Adelstein, J. and B. Sekulic, *Performance and reliability of a 1 kW amorphous Si photovoltaic*

roofing system, in *Conference Record of the IEEE Photovoltaic Specialists Conference*. 2005.

20. Dark, M.L., *A photovoltaics module for incoming science, technology, engineering and mathematics undergraduates. July, 20 at 20:33 2011*. 2011.
21. Durisch, W., A. Worz, and W. Plapp, *Characterisation of phtovoltaic generators.* Applied Energy, 2000. **273**(84): p. 1-4.
22. Ventre, R.M.A.J., *Photovoltaic systems engineering. CRC press LLC.* Boca Raton. smart Grid and Renewable Energy, 2000.
23. Cengiz, M.S.a.M.S.M., *Price-efficiency relationship for photovoltaic systems on a global basis. International Journal of Photoenergy, 2015. 2015(1): p. 256101*. 2015.
24. Rehman Kamal, M.A. and M. Nayel, *Performance characteristic of a PV module as influenced by dust accumulation: theory versus experiment.* Journal of Engineering and Applied Science, 2023.
25. Macabebe, E.Q.B., C.J. Sheppard, and E.E.J.S.E. Van Dyk, *Parameter extraction from I-V characteristics of PV devices.* 2011. **85**: p. 12-18.
26. Rummel, S. and T. McMahon, *Effect of cell shunt resistance on PV module performance at reduced light levels*, in *AIP conference proceedings*. 1996, American Institute of Physics.
27. Polverini, D., et al., , *A validation study of photovoltaic module series resistance determination under various operating conditions according to IEC 60891. 2012. 20(6): p. 650-660.* 2012.
28. Van Dyk, E. and E.L.J.R.E. Meyer, *Analysis of the effect of parasitic resistances on the performance of photovoltaic modules.* 2004. **29**: p. 333-344.
29. Lal, M., S.J.S.E.M. Singh, and S. Cells,, *A new method of determination of series and shunt resistances of silicon solar cells. 2007. 91(2-3): p. 137-142.* 2007.
30. Handy, R.J.S.-S.E., *Theoretical analysis of the series resistance of a solar cell. 1967. 10(8): p. 765- 775.* 1976.
31. Brecl, K., M.J.P.i.p.R. Topič,, *Applications and Simulation of losses in thin-film silicon modules for*

different configurations and front contacts. 2008. 16(6): p. 479-488. 2008.

32. Wenham, S.R., et al.,, *Applied photovoltaics. 2013: Routledge.* 2013.
33. Meyer, E.L. and O.K.J.C.E. Overen, *Blue skies and red sunsets: Reliability of performance parameters of various pn junction photovoltaic module technologies.* 2019. **6**.
34. Gottschalg, R., et al., , *The effect of spectral variations on the performance parameters of single and double junction amorphous silicon solar cells. 2005. 85(3): p. 415-428.* 2005.
35. Saive, R., *S-shaped current–voltage characteristics in solar cells: a review. IEEE Journal of Photovoltaics, 2019. 9(6): p. 1477-1484.* 2019.

36. Shockley, W., *Electrons and holes in semi conductors Van Nostrand Cie NY, 1950 [17] MILLER GL The Physics of Semi conductor Radiation Detectors Brookhaven Lecture*.
37. Green, M.A.J.E.C., *Solar cells: operating principles, technology, and system applications.* 1982.
38. Messenger, R. and J.J.P.L. Ventre, *Photovoltaic Systems Engineering*. 2000, Boca Raton.
39. Makrides, G., *Analysis of photovoltaic system performance time series: Seasonality and performance loss. Renewable Energy.* 2015. **77**: p. 51-63.
40. Merten, J., *Improved Equivalent Circuit and Analytical Model for Amorphous Silicon Solar Cells and Modules.* IEEE Xplore, 1998.
41. Hassan, Q., et al.,, *The PV cell temperature effect on the energy production and module efficiency.*
42. Ruch, P., *Effects of radiative forcing of building integrated photovoltaic systems in different urban climates.* Solar Energy, 2017. **147**: p. 399-405.
43. Ruch, P., *Effects of radiative forcing of building integrated photovoltaic systems in different urban climates. Solar Energy.* 2017. **147**: p. 399-405.
44. Prol, L. and K. Steinninger, *Photovoltaic self-consumption regulation in Spain: Profitability analysis and alternative regulation schemes. Energy Policy.* 2017. **108**: p. 742-754.
45. Badran, G.a.M.D., *Potential induced degradation in photovoltaic modules: A review of the latest research and developments. in Solar. 2023. MDPI.*
46. Bharadwaj, P., K. Karnataki, and V. John., *Formation of hotspots on healthy PV modules and their effect on output performance. in 2018 IEEE 7th world conference on photovoltaic energy conversion (WCPEC)(A joint conference of 45th IEEE PVSC, 28th PVSEC & 34th EU PVSEC). 2018. IEEE.* 2018.
47. Saidan, M., *Experimental study on the effect of dust deposition on solar photovoltaic panels in desert environment.* Renewable Energy, 2016. **92**: p. 499-505.
48. Qasem, H., et al.,, *Dust effect on PV modules. 2011.* 2011.
49. D.Jordan;C.Deline;S.Kurtz;M.kimball, *Robust PV Degradation Methodology.*
50. Köntges, M., et al., I, *Impact of transportation on silicon wafer-based photovoltaic modules.*
51. J.H.Wohlgemuth, *Standards for PV modules and Components. European Photovoltaic Solar Energy. Conference and Exhibition. Frankfurt, Germany. September 24–28, 2012., 2012, 2012.* 2012.
52. Dirnberger, D., *Photovoltaic module measurement and characterization in the laboratory. The Performance of Photovoltaic (PV) Systems*. 2017: Woodhead Publishing.
53. A. Augusto, H., S. Y., King, R. R., Bowden, S. G., and Honsberg, C.,, *Analysis of the recombination mechanisms of a silicon solar cell with low bandgap-voltage offset. Journal of*

Applied Physics, vol. 121, no. 20, p. 205704, 2017., 2017. 2017.

54. Csanyi, E., *Short Circuit Electrical Currents. Energy and Power journal*. 2010.
55. Hargrave, A., M.J. Thompson, and B. Heilman, *Beyond the knee point: A practical guide to CT saturation*, in *71st Annual Conference for Protective Relay Engineers (CPRE)*. 2018, IEEE.
56. Tress, W., *Interpretation and evolution of open-circuit voltage, recombination, ideality factor and subgap defect states during reversible light-soaking and irreversible degradation of perovskite solar cells.* Energy & Environmental Science, 2018. **11**(1): p. 151-165.
57. Hansen, B., *Understanding Maximum Power Points (MPP)*.
58. Qu, H.a.L.X., *Temperature dependency of the fill factor in PV modules between 6 and 40 C.*

. Journal of Mechanical Science and Technology, 2019. 33(4): p. 1981-1986.

, 2019.

59. Honsberg, C.a.B.J.U.h.w.p.o.p.s.-c.-o.B., *Solar Cell Operation 2016.* 2016.
60. Brano, V.L., et al., *„ An improved five-parameter model for photovoltaic modules. 2010. 94(8): p. 1358-1370. 2010.* 2010.
61. El-Shaer, A., M. Tadros, and M. Khalifa, *Effect of light intensity and temperature on crystalline silicon solar modules parameters.* International Journal of Emerging Technology and Advanced Engineering, 2014. **4**(8): p. 311-318.
62. Haynes, J. and W. Shockley, *The mobility of electrons in silver chloride.* Physical Review, 1951.
63. Sze, S.M., Y. Li, and K.K. Ng, *Physics of semiconductor devices*. Vol. 2021. John wiley & sons.
64. Rodrigues, E., et al. , *Simulation of a solar cell considering single-diode equivalent circuit model. in*

International conference on renewable energies and power quality, Spain. 2011. 2011.

65. Shen, Y., *IEC Standards for Electronic and Electrical Products: A Complete Guide.* Journal of IEC.
66. Alshadafan, A.F.I.A.F., *Governance and Inclusiveness of International Standard-Setting: The Case of the International Electrotechnical Commission*. 2023.
67. Salamah, T., *Effect of dust and methods of cleaning on the performance of solar PV module for different climate regions: Comprehensive review.* 2022. **827**.
68. Chamberlin, C.E., et al.,, *Effects of mismatch losses in photovoltaic arrays. 1995. 54(3): p. 165-171.* 1995.
69. Hussain Al Mahdi, P.G.L. and A.P. Mohammad Alghoul, *A Review of Photovoltaic Module Failure and Degradation Mechanisms: Causes and Detection Techniques. Power Electronics Architectures and Associated Control for Efficient and Reliable Solar PV Systems*. 2024.
70. Kumari, N., S.K. Singh, and S. Kumar,, *Effect of degradations and their possible outcomes in PV*

cells.

Renewable Energy Systems: Modeling, Optimization and Applications, 2022: p. 469-515. 2022.

71. Hernández-Callejo, L., S. Gallardo-Saavedra, and V. Alonso-Gómez, , *A review of photovoltaic systems: Design, operation and maintenance. Solar Energy, 2019. 188: p. 426-440.*
72. Segbefia, O.K., A.G. Imenes, and T.O.J.S.E. Saetre,, *Moisture ingress in photovoltaic modules: A review. 2021. 224: p. 889-906.* 2021.
73. Segbefia, O.K., A.G. Imenes, and T.O.J.S.E. Saetre,, *Solar cell degradation: the role of moisture ingress. 2023.* 2023.
74. Taylor, R., *Potential ecological impacts of ground-mounted photovoltaic solar panels. An introduction and literature review*. 2019.
75. Sayyah, A., M.N. Horenstein, and M.K.J.S.E. Mazumder, , *Energy yield loss caused by dust deposition on photovoltaic panels. 2014. 107: p. 576-604.* 2014.
76. Sulaiman, S.A., *Effects of Dust on the Performance of PV Panels.* 2011. **58**: p. 588-593.
77. Santhakumari, M., N.J.R. Sagar, and S.E. Reviews,, *A review of the environmental factors degrading the performance of silicon wafer-based photovoltaic modules: Failure detection methods and essential mitigation techniques. 2019. 110: p. 83-100.* 2019.
78. Wybo, J.-L.J.R.a.s.e.r., *Large-scale photovoltaic systems in airports areas: safety concerns. 2013. 21: p. 402-410.* 2013.
79. Pingel, S., *Potential induced degradation of solar cells and panels,* in *35th IEEE Photovoltaic Specialists Conference*. 2010, IEEE.
80. Domanski, K., *Systematic investigation of the impact of operation conditions on the degradation behaviour of perovskite solar cells.* Nature Energy, 2018. **3**(1): p. 61-67.
81. Grossiord, N., *Degradation mechanisms in organic photovoltaic devices.* Organic Electronics, 2012. **13**(3): p. 432-456.
82. Ndiaye, A., *Degradations of silicon photovoltaic modules: A literature review. Solar Energy*. 2013. **96**: p. 140-151.
83. Bouraiou, A., *Field investigation of PV pumping system ageing failures operation under Saharan environment.* 2022. **243**: p. 142-152.
84. Zuboy, J., *Getting Ahead of the Curve: Assessment of New Photovoltaic Module Reliability Risks Associated with Projected Technological Changes*. 2022.
85. Gao, L., et al., , *Parallel-connected solar PV system to address partial and rapidly fluctuating shadow conditions. IEEE Transactions on industrial Electronics, 2009. 56(5): p. 1548-1556.* 2009.
86. Bonnet-Eymard, M., et al., , *Optimized short-circuit current mismatch in multi-junction solar*

cells.

Solar energy materials and solar cells, 2013. 117: p. 120-125. 2013.

87. Lisemumbai, *Chapter number 3.0. PV modules explained. The Indian Institute of Solar Energy, 2023.* 2023.

88. Das, P., *Different Degradation Modes of Field-Deployed Photovoltaic Modules: A Literature Review. Applications of Computational Intelligence in Management & Mathematics*. 2023.

89. Sharma, S. and P. Malik, *Vikrant Sharma & Sunanda Sinha, Different Degradation Modes of PV Modules: An Overview.* Advancements in Nanotechnology for Energy and Environment, 2022.

90. Vieira, R.G., et al., , *A comprehensive review on bypass diode application on photovoltaic modules.*

Energies, 2020. 13(10): p. 2472. 2020.

APPENDICES

Appendix I: Calculations of efficiencies of modules found at different schools

(i) Calculation of modular area

The length, L and width, W, of the module were measured using a tape measure. The area A is calculated from the formula, $A = L \times W$.

$A = 1.23 \times 0.66 = 0.8118\ m^2$

(ii) Calculation of efficiencies for each module per school.

The formula $\eta = \frac{P_{max}}{A \times G} \times 100\%$ was used.

(a) Orungo High School

Before Wash

Module A $\eta = \frac{37.49}{1000 \times 0.8118} \times 100\% = 4.62\%$

Module B $\eta = \frac{35.82}{1000 \times 0.8118} \times 100\% = 4.41\%$

Module AB $\eta = \frac{39.77}{1000 \times 0.8118} \times 100\% = 4.90\%$

Module Aw $\eta = \frac{57.52}{1000 \times 0.8118} \times 100\% = 7.09\%$

Module Bw $\eta = \frac{54.51}{1000 \times 0.8118} \times 100\% = 6.71\%$

Module ABw $\eta = \frac{61.88}{1000 \times 0.8118} \times 100\% = 7.62\%$

(b) Katine S S

Module A $\eta = \frac{21.84}{1000 \times 0.8118} \times 100\% = 2.69\%$

Module B $\eta = \frac{8.64}{1000 \times 0.8118} \times 100\% = 1.06\%$

Module AB $\eta = \frac{22.37}{1000 \times 0.8118} \times 100\% = 2.76\%$

Module Aw $\eta = \frac{34.6}{1000 \times 0.8118} \times 100\% = 4.26\%$

Module Bw $\eta = \frac{20.88}{1000 \times 0.8118} \times 100\% = 2.57\%$

Module ABw $\eta = \frac{40.04}{1000 \times 0.8118} \times 100\% = 4.9\%$

(c) Akii Bua comprehensive SS

Module A $\eta = \frac{5.57}{1000 \times 0.8118} \times 100\% = 0.69\%$

Module Aw $\eta = \frac{18.74}{1000 \times 0.8118} \times 100\% = 2.3\%$

Module B $\eta = \frac{5.86}{1000 \times 0.8118} \times 100\% = 0.72\%$

Module Bw $\eta = \frac{6.84}{1000 \times 0.8118} \times 100\% = 0.84\%$

String AB $\eta = \frac{19.64}{1000 \times 0.8118} \times 100\% = 2.4\%$

String ABw $\eta = \frac{34.71}{1000 \times 0.8118} \times 100\% = 4.28\%$

(d) Adwari ss

Module A $\eta = \frac{35.84}{1000 \times 0.8118} \times 100\% = 4.41\%$

Module Aw $\eta = \frac{37.8}{1000 \times 0.8118} \times 100\% = 4.66\%$

String AB $\eta = \frac{36.10}{1000 \times 0.8118} \times 100\% = 4.45\%$

String ABw $\eta = \frac{36.71}{1000 \times 0.8118} \times 100\% = 4.52\%$

Appendix II: Visual inspection checklist by International Electrotechnical Commission (IEC)

		Defect Present?		
Component	Defect	No	Yes	Defects Present
21. Label	21.1. Missing			
	21.2. Poorly attached			
	21.3. Information is missing			
	21.4. Incorrect spelling			

22. Back Sheet	22.1. Burn makes			
	22.2. Discolouration			
23. Junction Box	23.1. Faulty electrical connection			
	23.2. Cracks/breaks/gaps in housing			
	23.3. Sealant Failure			

	23.4. Electrical polarity not indicated			
24. Wiring	24.1. Cracks or exposed metal			
25. Frame	25.1. Damaged			
	25.2. Adhesive/sealant failure			
26. Front Glass	26.1. Cracks			

27. Encapsulation	27.1. Discoloration			
28. Cells	8.2. Snail trails			
	8.3. Shiny locally/inconsistent colour			
29. Cell Metallization	29.1. Fingers not connected to bus bar			

	29.2. Not the same pattern on all cells			
	29.3. Fingers off the edge of corner of the cells			
30. Cell Interconnection	30.1. Interconnection is discontinuous			
	30.2. Poorly aligned and/or soldered			

Appendix III: Manufacturer's efficiency

The manufacture's efficiency was calculated from the formula,

$$\eta = \frac{P_{\max}}{A \times G} \times 100\%.$$

Given Pmax = 110 w

Area, A of the module = 0.8118 m^2

Irradiance, G =1000 wm^2

$$\eta = \frac{110}{1000 \times 0.8118} \times 100\%$$

= 13.6 %